SAN FRANCISCO ESTUARY & WATERSHED SCIENCE
Sponsored by the Delta Science Program and the UC Davis Muir Institute

SEPTEMBER 2019

RESEARCH

Effects of Drought and the Emergency Drought Barrier on the Ecosystem of the California Delta

Wim Kimmerer,[1]* Frances Wilkerson,[1] Bryan Downing,[2] Richard Dugdale,[1] Edward S. Gross,[3] Karen Kayfetz,[4] Shruti Khanna,[5] Alexander E. Parker,[6] Janet Thompson[7]

ABSTRACT

In 2015, the fourth year of the recent drought, the California Department of Water Resources installed a rock barrier across False River west of Franks Tract to limit salt intrusion into the Delta at minimal cost in freshwater. This Barrier blocked flow in False River, greatly reducing landward salt transport by decreasing tidal dispersion in Franks Tract. We investigated some ecological consequences of the Barrier, examining its effects on water circulation and exchange, on distributions of submerged aquatic vegetation (SAV) and bivalves, and on phytoplankton and zooplankton. The Barrier allowed SAV to spread to areas of Franks Tract that previously had been clear. The distributions of bivalves (*Potamocorbula* and *Corbicula*) responded to the changes in salinity at time-scales of months for newly settled individuals, to 1 or more years for adults, but the Barrier's effect was confounded with that of the drought. Nutrients, phytoplankton biomass, and a *Microcystis* abundance index showed little response to the Barrier. Transport of copepods — determined using output from a particle-tracking model — indicated some intermediate-scale reduction with the Barrier in place, but monitoring data did not show a larger-scale response in abundance. These studies were conducted separately and synthesized after the fact, and relied on reference conditions that were not always suitable for identifying the Barrier's effects. If barriers are considered in the future, a modest program of investigation should be undertaken that includes adequate replication and ensures that suitable reference conditions are available to allow barrier effects to be distinguished unambiguously from other sources of variability.

SFEWS Volume 17 | Issue 3 | Article 2

https://doi.org/10.15447/sfews.2019v17iss3art2

* Corresponding author: *kimmerer@sfsu.edu*

1 Estuary & Ocean Science Center
San Francisco State University
Tiburon CA 94920 USA

2 U.S. Geological Survey
Sacramento, CA 95819 USA

3 Resource Management Associates, Inc.
Walnut Creek, CA 94596 USA and
University of California, Davis
Davis, CA 95616 USA

4 Delta Stewardship Council
Sacramento, CA 95814 USA

5 California Department of Fish and Wildlife
Sacramento, CA 95206 USA

6 California State University Maritime Academy
Vallejo, CA 94590 USA

7 U.S. Geological Survey
Menlo Park, CA 94025 USA

KEY WORDS

hydrodynamics, box model, tidal barrier, copepod, water quality, phytoplankton, submerged aquatic vegetation, bivalve

INTRODUCTION

The California (Sacramento–San Joaquin) Delta (Figure 1) is the hub of much of California's water supply, where water from reservoirs to the north is routed to farms and cities in and south of the Delta and to the San Francisco Estuary (the estuary). When Delta outflow is low because of low river inflow and high export flow, ocean-derived salts can penetrate into the Delta, reducing the quality of exported water. Water quality can degrade to the point that regulatory guidelines are exceeded and exports must be curtailed. To prevent this, enough water must be allowed to flow through the estuary ("outflow") to maintain the estuarine salinity field far enough seaward to keep saline water out of water intakes.

Franks Tract (Figure 1A), in the west Central Delta, accelerates the tidal penetration of salt into the Delta: on the flood, the water from False River (FR in Figure 1B) enters Franks Tract as a jet (or "nozzle"), flowing across the Tract and carrying salt with it (MacWilliams et al. 2016). On the following ebb, the water flows out from all parts of Franks Tract, such that the water leaving Franks Tract on the ebb is, on average, fresher than the water entering on the flood. This process combines "tidal pumping" and "tidal trapping" (Fischer et al. 1979) in a dispersive process that brings salt into Franks Tract, thus increasing salinity in the water that flows toward the export facilities in the Southern Delta.

Operable gates, such as the Delta Cross Channel (DCC) gates (Figure 1), and temporary barriers have been used to alter flow pathways in the Delta to improve water quality and water-supply reliability at the South Delta pumping plants and other locations. Under most summer conditions, outflow is adequate to limit salt intrusion to the Western Delta or further west — minimizing the addition of salt to exported water — but can require releases of water from reservoirs that further deplete dwindling supplies.

The year 2015 was the fourth year of a severe drought in much of California. The 2015 snowpack was the lowest in 500 years, and the 2014–2015 winter was the warmest on record as of 2015, which exacerbated the effects of low precipitation on water supply to reservoirs (Berg and Hall 2017). Water years (which begin 1 October of the previous calendar year) 2014 and 2015 were designated critically dry, with reservoirs throughout California at only 26% of capacity (*http://engaging-data.com/ca-reservoir-level/*), and flows through the pumping plants in the Southern Delta (Figure 1A) were the lowest since the State Water Project became fully operational in 1973 (Figure 2).

In 2015, the California Department of Water Resources (CDWR) installed a temporary rock barrier (hereafter, the Barrier) that spanned 230 m across west False River in the Central Delta, just west of Franks Tract (FR, Figure 1B). An essential part of CDWR's drought response, this Barrier allowed CDWR to reduce Delta outflow, thereby saving water in the reservoirs while meeting water-quality standards and minimizing salination of exported water. The Barrier was constructed in May 2015 and the channel was closed on 28 May; the Barrier was breached on 1 October 2015, and fully removed by 15 November 2015 (Figure 3).

The Barrier reduced the Delta outflow needed to limit salt intrusion into the Delta by reducing tidal dispersion across False River and Franks Tract. Net Delta outflow was similar between 2015 and other dry years, particularly 2014 (Figure 3). Salinity at Jersey Point, west of Franks Tract (California Data Exchange Center, CDEC station SJJ, Figure 1), was higher in 2015 than in 2014 (Figure 3A), and salinity at Old River to the north of Franks Tract (CDEC station OSJ) was proportionately higher (Figure 3B). However, salinity at Holland Cut on Old River south of Franks Tract (CDEC station HOL) during 2015 was nearly identical to that in 2014 (Figure 3C). Thus, the Barrier was successful in keeping salinity below water-quality standards in a primary waterway that leads to the water export facilities.

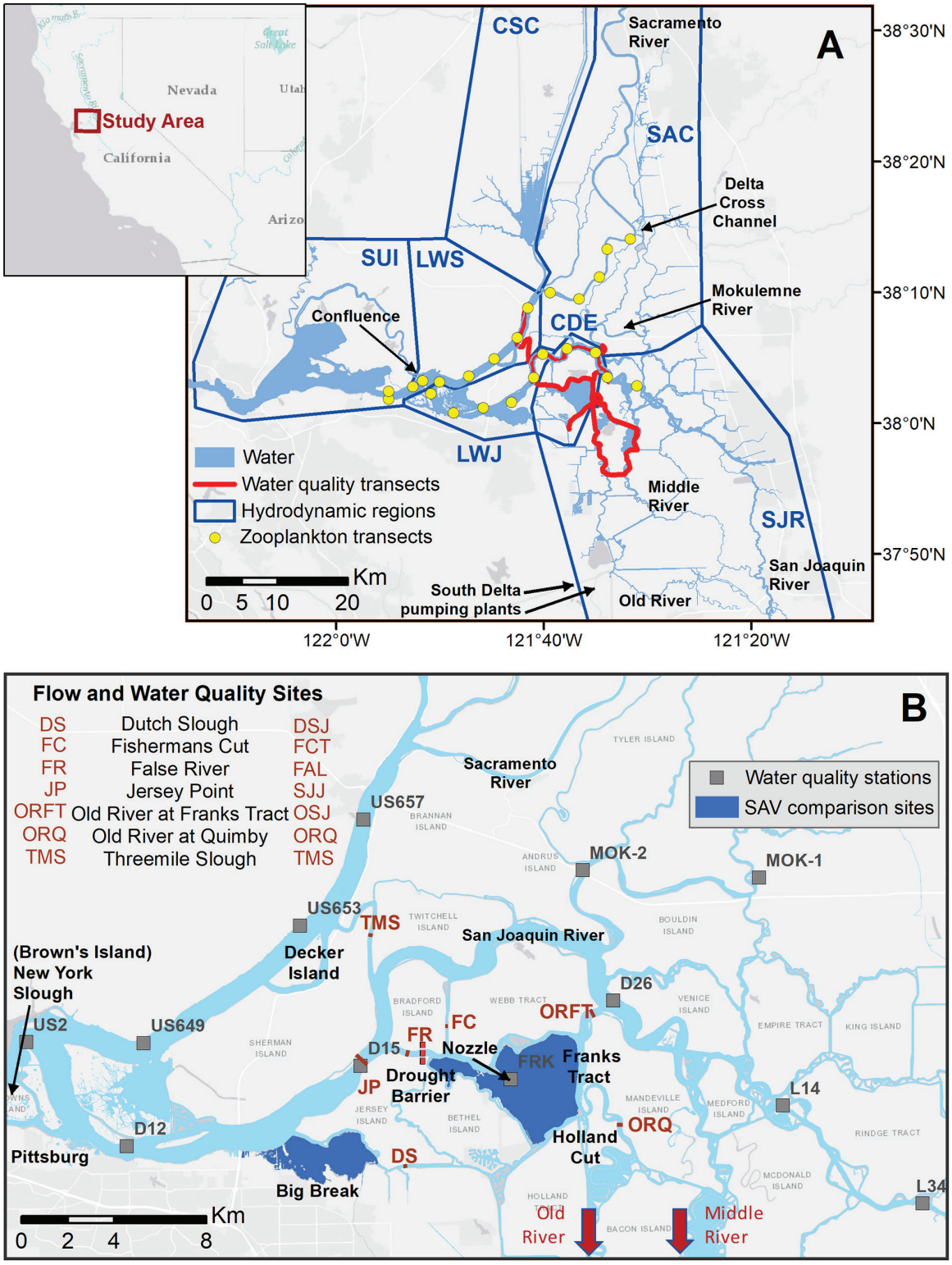

Figure 1 Maps of the study area including general locations of investigations, locations discussed in the text, sampling stations, and transects, with inset showing general location. (**A**) Delta and Suisun Bay; *3-letter codes* and *lines* identify boundaries of boxes used in the hydrodynamic box model. (**B**) Study area of Western Delta including Franks Tract; flow and water-quality sites are listed by their USGS station identifiers (flow, *left*) and California Data Exchange Center (CDEC) station identifiers (water quality, *right*).

https://doi.org/10.15447/sfews.2019v17iss3art2

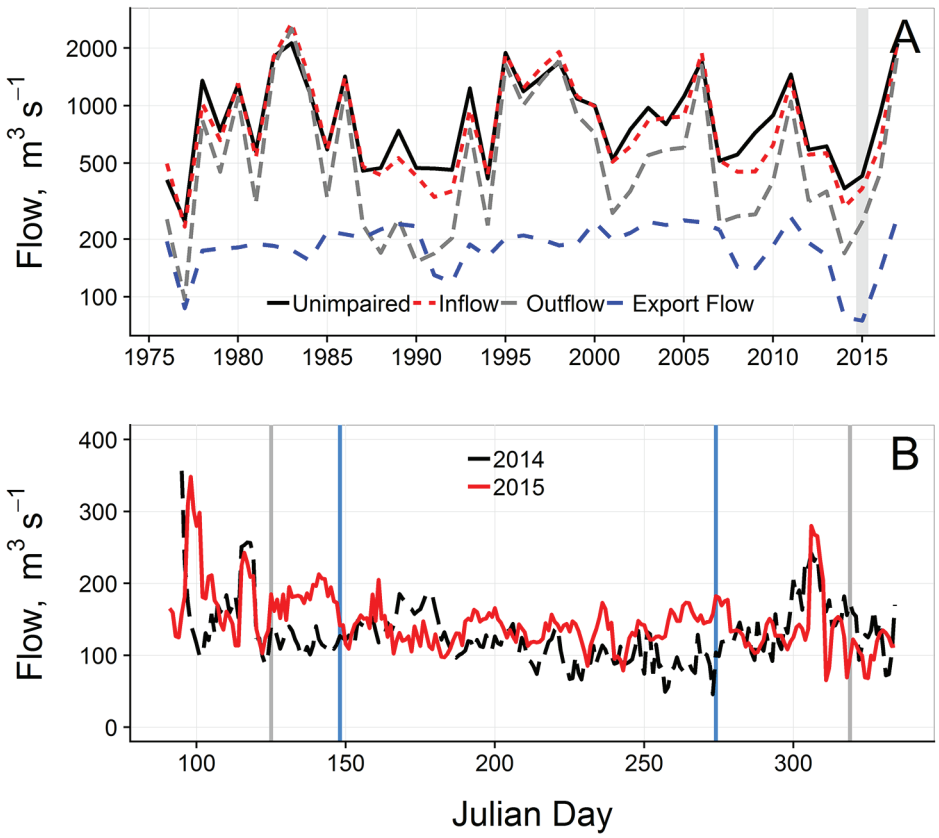

Figure 2 Flow variables for recent years. (**A**) unimpaired flow (natural flow to the watershed without infrastructure), Delta inflow and outflow, and export (diversion) flow from the South Delta, all means by water year (October-September), with 2015 highlighted by *vertical gray line*. (**B**) daily outflow for 2014 and 2015; *vertical lines* indicate timing of beginning and end of Barrier construction (*gray*) and of full blockage of False River by the Barrier (*blue*). Source: unimpaired flow from *http://cdec.water.ca.gov/cgi-progs/iodir/WSIHIST*, and other flows from the Dayflow flow-accounting program (*http://www.water.ca.gov/dayflow/*).

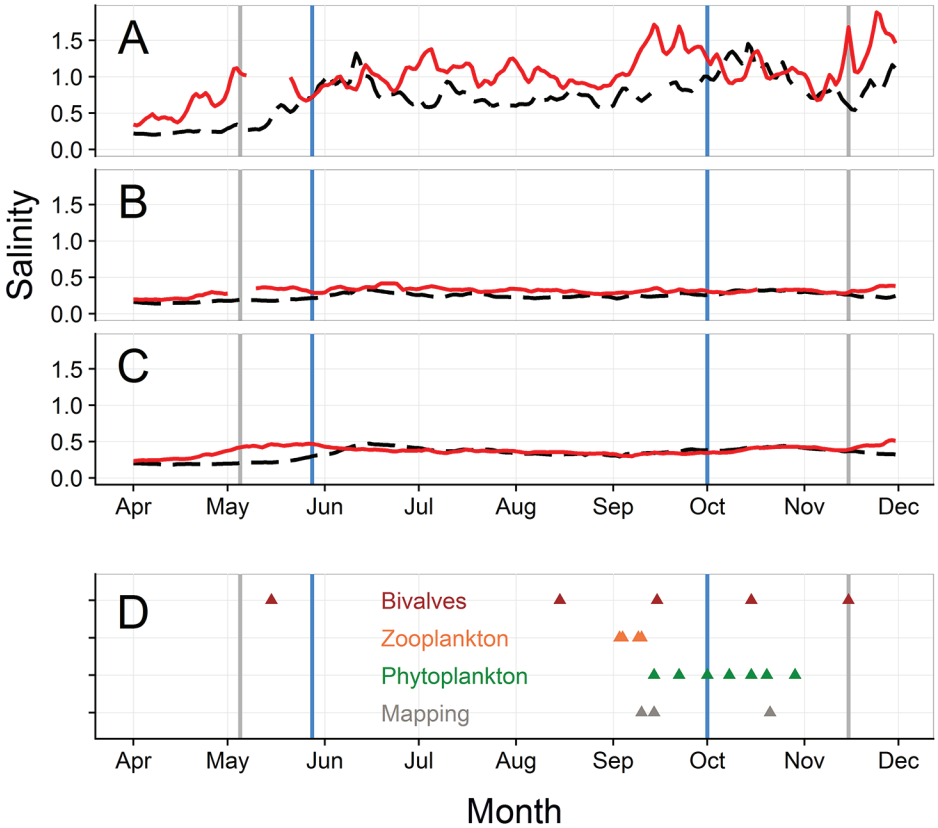

Figure 3 Salinity in the vicinity of Franks Tract with and without the Barrier (locations in Figure 1). (**A**) Jersey Point in 2014 (*black dashed*) and 2015 (*red solid*); (**B**) as in (**A**) for Old River north of Franks Tract; (**C**) as in (**A**) for Old River south of Franks Tract;, (**D**) timeline of sampling events in this study, excluding samples from other years (see Table 1 and text). *Vertical lines* indicate timing of beginning and end of Barrier construction (*gray*) and of full blockage of False River by the Barrier (*blue*). Source: Data from CDEC (*http://cdec.water.ca.gov/*) and NWIS (*https://waterdata.usgs.gov/nwis*).

Table 1 Summary of key anticipated effects of the Barrier and whether they were supported by evidence developed during this study

Topic	Anticipated difference barrier - reference	Evidence
Movement of water & particles	Reduced tidal currents in False River, increased in other areas	Yes
	Reduced exchange & salt transport between west and central Delta	Yes
	Altered patterns of salinity at intermediate scale	Yes
Zooplankton	Reduced transport between central Delta and points west	Yes
	Reduced abundance in Low-Salinity Zone	No
Submerged aquatic vegetation	Higher SAV in the middle of Franks Tract	Yes
	No change in SAV in Big Break reference site	Yes
Water quality & age	Altered patterns of water age, nitrate and water quality	No
Nutrients & phytoplankton	Increase in phytoplankton blooms in Franks Tract	No
	Increase in *Microcystis* in Franks Tract	No
Bivalves	Increased penetration of *Potamocorbula* into Delta	Yes
	Increased bivalve grazing rate in areas of elevated salinity in confluence	Yes
	Increased bivalve recruitment near confluence	Yes

Research team members anticipated several of the Barrier's consequences, including some that had potential ecological ramifications. (Table 1). First, they expected the reduction in longitudinal dispersion to reduce the longitudinal transport of organisms and other substances in addition to salt. These may have included plankton such as copepods and larval clams. Second, the alteration of tidal velocities in channels of the western Delta could have altered the suitability of habitat for submerged aquatic vegetation (SAV). Third, the change in tidal and net velocities was expected to alter local water age in the Delta, possibly altering conditions for accumulation of phytoplankton including the toxigenic species *Microcystis aeruginosa*.

Generally, effects of the Barrier were expected at the local scale (i.e., the immediate vicinity of the Barrier), and possibly at the intermediate scale (around False River and Franks Tract and their connections to other waterways), and the large scale of the entire northern estuary (Figure 1A). Except as described below, we focused our investigations at the intermediate to large scale, and we did not examine small-scale local effects.

Here we describe and synthesize results from investigations designed to detect and quantify ecological changes that resulted from the installation of the Barrier. We do not address the short-term, small-scale effects of installation and removal, but rather the effects of having the Barrier in place, including effects remaining after it was breached. The evidence for effects necessarily rests on an unreplicated study, in that the Barrier was in place during only 1 year. Although data from other recent dry years were useful for comparisons, no 2 years are identical, and any differences could not be unequivocally attributed to the Barrier, so these comparisons are imperfect and formal statistical tests are generally inappropriate. Therefore, we used a weight-of-evidence approach to attempt to distinguish the

https://doi.org/10.15447/sfews.2019v17iss3art2

effects of the Barrier from those of the drought, in the context of high variability. We show below that the inferred ecological effects of the Barrier were generally modest to negligible.

The investigations described here were proposed and funded as separate research projects; because each had its own objectives and research questions, they have different spatial and temporal scopes, and different reference conditions based on availability of data (Table 2, Figure 1). This synthesis was not begun until the projects had been largely completed. Therefore, we have organized this paper as a series of brief sections that describe each project and its findings, followed by a section that synthesizes the Barrier's overall ecological effects. In each section and the synthesis below, we describe the Barrier's effects as changes from one or more reference conditions or baselines. The baselines and years for comparison varied by topic, reflecting availability of comparable data (Table 2). Each section below gives a very brief synopsis of methods, which are described in detail in Appendix A.

MOVEMENT OF WATER AND PARTICLES

The expected effects of the Barrier on hydrodynamics were decreased tidal prism in False River, decreased salt intrusion into Franks Tract via False River, and increased tidal prism in Fisherman's Cut (Figure 1). The Barrier imposed a longer path for oceanic salt intrusion into the South Delta, with expected decreases in South Delta salinity for a given set of inflows and exports. The larger-scale influence of the Barrier on hydrodynamics and salt intrusion processes was uncertain.

We applied the UnTRIM model (Casulli and Walters 2000; Casulli and Stelling 2011) to simulate three-dimensional hydrodynamics from the Pacific Ocean through the estuary (Andrews et al. 2017) and to investigate flow patterns in the estuary, focusing on the western Delta, with and without the Barrier. We then set up a spatial box model that spanned the Delta and Suisun Bay, and used a particle-tracking model driven by hydrodynamic model results to determine elements of a matrix that showed the probability that a particle in one box would be in the same or a different box, or lost from the system, after 1 day. This exchange matrix was then used to calculate movement rates of copepods (see "Zooplankton") for representative conditions with and without the Barrier. We estimated the movement between regions both for passive particles and particles with a vertical tidal migration behavior that represented that of the copepod *Pseudodiaptomus forbesi* (Kimmerer et al. 2014). Additional information on the hydrodynamic and particle-tracking model scenarios is available in Appendix A; Appendix B provides information on hydrodynamic model calibration.

Table 2 Individual projects investigating the effects of the Barrier in 2015, including topic, lead authors, spatial and temporal scope, and years with available data for comparison

Topic	Leads	Spatial scope	Temporal scope	Comparison years
Movement of water & particles	Gross, Kimmerer	Entire estuary	Synthetic flows	—
Zooplankton	Kimmerer, Gross	Central Delta, Suisun Bay	Sept 2015	2010–2012
Submerged aquatic vegetation	Khanna	Franks Tract, Big Break	Sept 2015 Imagery	2004, 2016
Water quality and age	Downing	Entire Delta	Sept–Oct 2015	2016
Nutrients & phytoplankton	Wilkerson, Dugdale, Parker	Central Delta	Sept–Oct 2015	2005–2016
Bivalves	Thompson	Delta and Suisun Bay	May, Aug, Sep, Oct, Nov	2007–2012, 2014–2016

Results and Discussion

The hydrodynamics and estimated exchange for the with-Barrier scenario used a flow of 115 $m^3 s^{-1}$, while the no-Barrier scenario used 138 $m^3 s^{-1}$, the estimated flow to maintain X2[1] at the same position with and without the Barrier (see Appendix A). The Barrier strongly influenced currents and salinity at the intermediate scale. The daily-averaged, depth-averaged tidal current speeds were higher in False River and in the "nozzle" that leads into Franks Tract without the Barrier (Figures 1 and 4). However, the lower flow in False River with the Barrier than without resulted in greatly increased tidal currents through Fisherman's Cut and Dutch Slough (Table 3). As expected, the predicted net (i.e., tidally averaged) flow was lower in False River and higher in Old River at Franks Tract with the Barrier, and differed only slightly at Jersey Point (Table 3), suggesting that differences in net flows with the Barrier were strongest at the intermediate scale. The modeled net flow at Fisherman's Cut was lower with the Barrier, despite a much larger tidal flow.

Hydrodynamic changes that resulted from the Barrier influenced the pathways and magnitude of predicted particle exchange between the Central and western Delta, but differences were small beyond the intermediate scale. The Barrier reduced exchange between the Central Delta region (CDE) and other regions for both passive and tidally migrating particles (Figure 5, Table 4). For regions far from the Barrier, exchange differed very little between the with-Barrier case and the no-Barrier case. Vertical tidal migration generally improved retention, leading to less

1 The distance from the mouth up the axis of the estuary to where the daily average near-bottom salinity is 2 (Jassby et al. 1995).

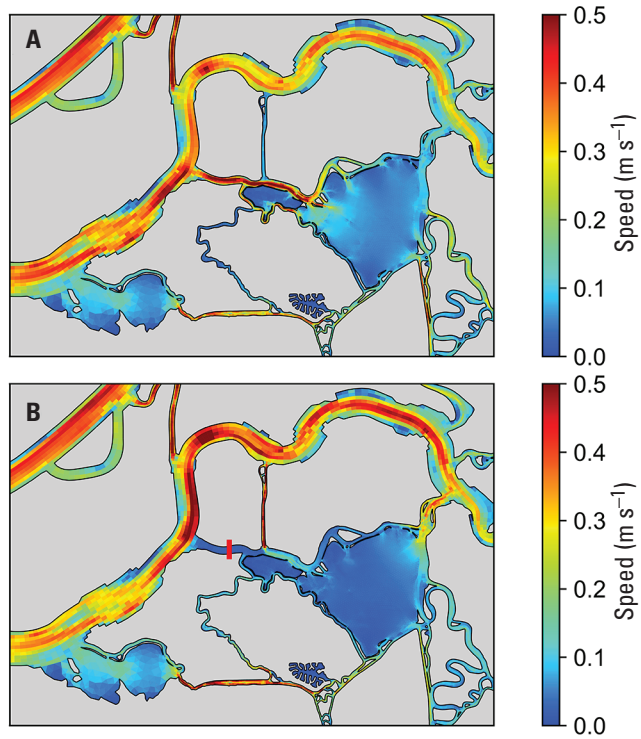

Figure 4 Daily averaged tidal current speed in and around False River and Franks Tract predicted from the hydrodynamic model for steady flow scenarios (**A**) without Barrier; (**B**) with Barrier.

Table 3 Root mean square (RMS) tidal flow ($m^3 s^{-1}$) and tidally averaged predicted net flow at locations surrounding Franks Tract (Figure 1B) for the no-Barrier and with-Barrier scenarios. The column labeled "Positive" provides the convention for positive flow direction at each location

	RMS tidal flow		Net flow		
Location	No barrier	With barrier	No barrier	With barrier	Positive
Dutch Slough	179.8	222.4	−4.3	−7.0	West
False River	966.9	48.9	5.5	1.1	West
Fishermans Cut	33.2	215.4	31.8	2.3	South
Jersey Point	2656.3	2354.3	85.0	90.8	Southwest
Old River Franks Tract	230.0	595.5	-6.4	−19.5	North
Old River at Quimby	13.5	160.5	−22.0	−13.5	North
Threemile Slough	645.5	608.4	17.5	24.9	South

https://doi.org/10.15447/sfews.2019v17iss3art2

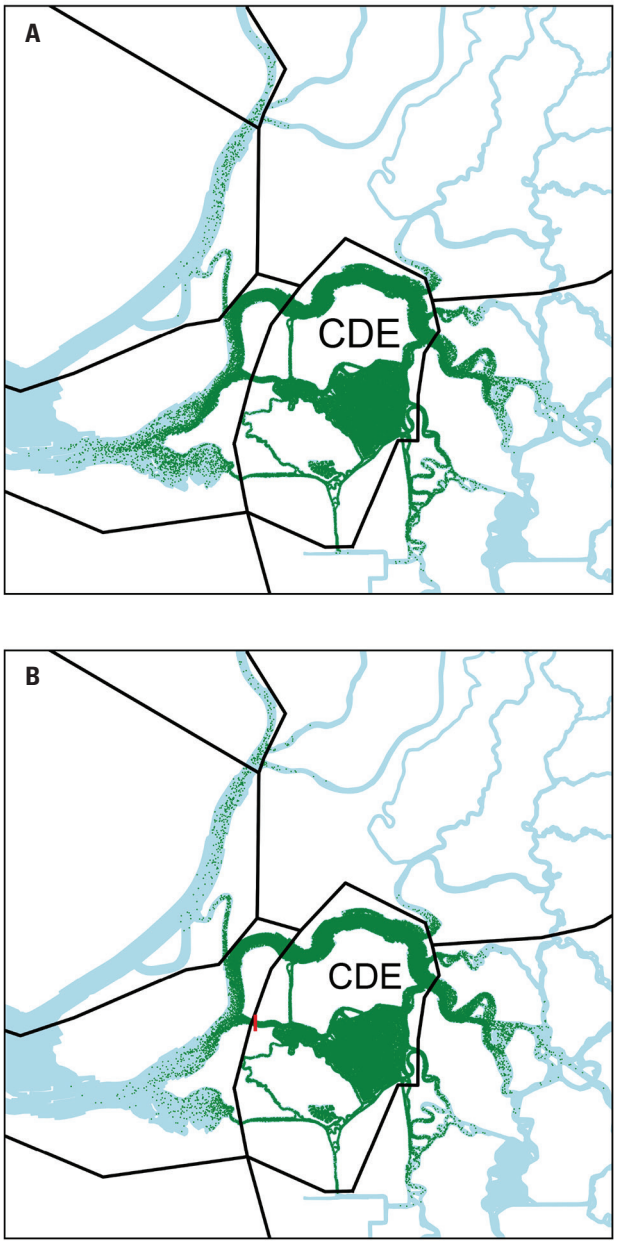

Figure 5 Final position of particles with biased tidal migration behavior, 1 day after release from the Central Delta (CDE) region. (**A**) without Barrier; (**B**) with Barrier.

exchange (loss) from source regions than occurs with passive behavior (Table 4). The largest effect of the Barrier in the box model was reduced exchange between the CDE and the lower San Joaquin River (LWJ) with the Barrier in place: from 0.13 d^{-1} to 0.09 d^{-1} for passive particles and 0.11 d^{-1} to 0.07 d^{-1} for vertically migrating particles (Table 4).

ZOOPLANKTON

The effects of the Barrier on zooplankton were expected to be greatest for the copepod *Pseudodiaptomus forbesi*, which makes up a large part of the diet of the endangered Delta Smelt *Hypomesus transpacificus* and other fishes in the low-salinity zone (LSZ) (Bryant and Arnold 2007; Slater and Baxter 2014). *P. forbesi* is most abundant in freshwater, and mortality of the young stages is high in brackish water, implying a subsidy of *P. forbesi* from freshwater to the LSZ, mediated mainly by dispersion due to tidal mixing (Kayfetz and Kimmerer 2017; Kimmerer et al. 2017, 2019). We anticipated that the change in dispersion caused by the Barrier would reduce the subsidy, and possibly lead to a reduced food supplyfor Delta Smelt in the LSZ (Table 1). The objectives of this study element were to use available data and new sampling to calculate abundance gradients, and use the abundance data with the box model output (see "Movement of Water and Particles") to determine how the Barrier affected the seaward transport of copepods.

The zooplankton analysis used exchange matrices from the box model together with field-collected data on abundance to estimate movement of *P. forbesi* between spatial boxes with and without the Barrier (Appendix A). We also used long-term monitoring data to determine whether changes in movement altered zooplankton abundance in the low-salinity habitat of Delta Smelt.

Results and Discussion

Transect data on the Sacramento River showed a steepening of the abundance gradients in 2015 compared with those from 2010 and 2012 (Figures 6A, 6C, and 6E), but this was mainly because maximum salinity was higher in 2015 than in the other years (by 5–6 salinity units on the Sacramento River and 2–3 on the San Joaquin River). This steepening resulted in changes in abundance within the boxes as estimated using the transect data (Figures 1A and 6). In the San Joaquin, Central Delta, and lower Sacramento boxes, and in part of the upper Sacramento box, abundance was generally higher in 2015 than in the other years; in the Suisun box, it was mostly lower than in other years.

Table 4 Fraction of particles from each source region ending in each destination including losses to sea and entrainment sinks (exports and consumption in Delta) for hydrodynamic scenarios with and without Barrier. All predicted exchange values lower than 0.01 are *blank*, and proportions of particles retained in each box are shown in *gray text*. Values given are for passive particles (*normal text*) or *bold* for particles that migrated tidally as in Kimmerer et al. (2014) where these differed from the passive case by more than 0.01 for either with-Barrier or no-Barrier case. The geographical extent of each source region is given in Figure 1A. SEA signifies seaward losses and SNK signifies losses to exports or consumptive use

Source	Barrier	SAC	CSC	SJR	CDE	LWS	LWJ	SUI	SEA	SNK
SAC	Yes	0.86	0.05	0.05	0.03	0.01				0.01
	No	0.86	0.06	0.05	0.02	0.01				0.01
CSC	Yes	0.04	0.89			0.07				
	No	0.03	0.89			0.07				0.01
SJR	Yes			0.93	0.05					0.02
	No			0.93	0.05					0.02
CDE	Yes			0.09 **0.06**	0.81 **0.86**	0.01	0.09 **0.07**			
	No			0.09	0.77 **0.81**	0.01	0.13 **0.11**			
LWS	Yes	0.01	0.03			0.68 **0.77**	0.16 **0.10**	0.13 **0.09**		
	No	0.01	0.02			0.65 **0.77**	0.18 **0.11**	0.14 **0.08**		
LWJ	Yes				0.05	0.14 **0.14**	0.78 **0.78**	0.03 **0.02**		
	No				0.07	0.14 **0.16**	0.76 **0.74**	0.04 **0.02**		
SUI	Yes					0.03 **0.05**	0.01	0.86 **0.88**	0.10 **0.05**	
	No					0.02 **0.05**	0.01	0.86 **0.90**	0.10 **0.04**	

Differences in exchange with and without the Barrier were strongest for pairs of boxes near and aligned with the Barrier, and weak elsewhere (see "Movement of Water and Particles"). The Barrier substantially reduced subsidies of copepods to some boxes, notably the lower San Joaquin box (LWJ) but also the Suisun box (Figure 7). The Barrier had a negligible effect on subsidies to the lower Sacramento (Figure 7) and other boxes (not shown).

Despite the differences in some of the local exchange terms between with-Barrier and no-Barrier cases, at the larger scale, the effect of the Barrier was not evident. Data from the Interagency Ecological Program's (IEP's) monitoring program showed that abundance of *P. forbesi* copepodites was, if anything, higher in 2015 than in other dry years (Figure 8). The median and range of predicted abundance for salinities that corresponded to the ranges where Delta Smelt are most abundant during summer and fall showed that, generally, *P. forbesi* copepodites were more abundant in these ranges in 2015 than in any other dry year.

SUBMERGED AQUATIC VEGETATION (SAV)

The reduction in current speeds within Franks Tract with the Barrier in place was expected to lead to a more lake-like environment, increasing the biomass of SAV and changing its distribution (Table 1). We expected species composition to remain as before the Barrier whereas, had salinity been higher, we would have expected a shift from freshwater species to more salt-tolerant species

https://doi.org/10.15447/sfews.2019v17iss3art2

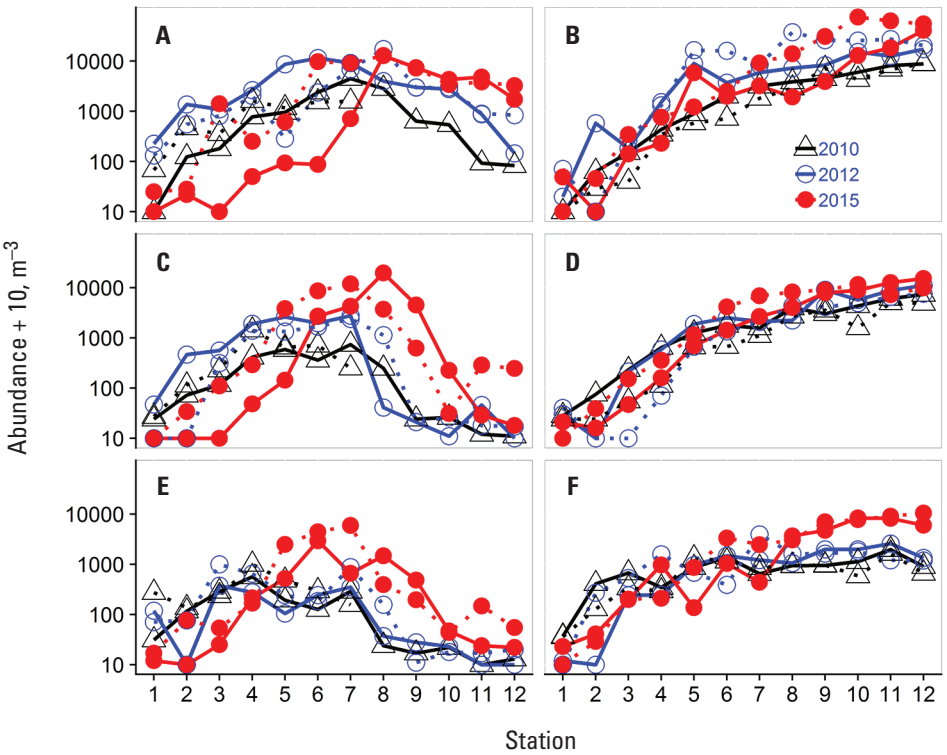

Figure 6 Abundance of major life stages of *Pseudodiaptomus forbesi* (**A**, **B**, nauplii; **C**, **D**, copepodites; **E**, **F**, adults) on transects up each river (**A**, **C**, **E**, Sacramento; **B**, **D**, **F**, San Joaquin) during two dry pre-Barrier years (2010 and 2012) and the Barrier year (2015). *Solid* and *dotted lines* distinguish separate transects in each year.

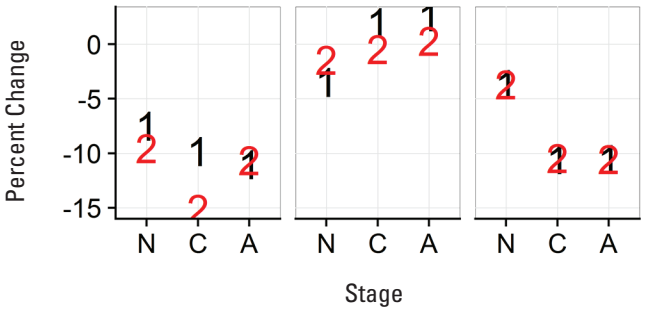

Figure 7 Percent change in copepod subsidies (rates of gain) by life stage in (**A**) the lower San Joaquin; (**B**) the lower Sacramento; and (**C**) Suisun boxes. Numbers refer to duplicate transects 1 and 2 in 2015, and stages are nauplii, copepodites, and adults.

such as Sago pondweed (*Stuckenia pectinata*). The objective of this study was to use remote sensing to compare SAV extent and distribution in Franks Tract pre- and post-Barrier to detect changes that could be attributed to the Barrier. To discriminate between the effect of the Barrier and that of drought and other factors acting on the Delta, we compared the response at Franks Tract to the response at Big Break (Figure 1B, label FC). This region has a lake-like environment similar to that of Franks Tract but lies west of the Barrier, where it is exposed to higher salinity than Franks Tract, and where the Barrier's effect would have been minimal.

We compared maps of SAV that were produced using airborne hyperspectral imagery over the Delta from summer of 2004 and fall of 2015–2017 to determine the Barrier's immediate effect on SAV extent and density. Image processing and field data collection for training and validation are described in Appendix A. We assessed accuracy through confusion matrices and kappa

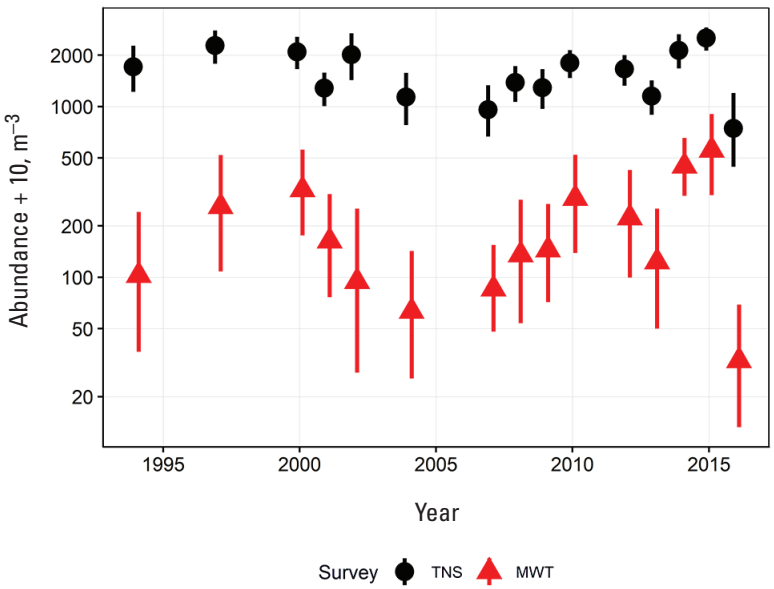

Figure 8 Abundance in LSZ of *P. forbesi* copepodites predicted by generalized additive models (GAMs) fitted to abundance data for each dry year. Values are medians and ranges of abundance predicted over the salinity ranges where resource selection functions for Selta Smelt exceed 80% of their maximum values (Kimmerer et al. 2013) for the summer townet survey (TNS) and the fall midwater trawl survey (MWT). GAMs were fitted to abundance (m^{-3}) vs. salinity with a log link function and variance proportional to the mean. Source: R Development Core Team 2015.

coefficients, and assessed SAV density by calculating a common vegetation index called Normalized Difference Vegetation Index (NDVI).

Results and Discussion

Accuracy was greater than 85% for all 3 years, and kappa was greater than 0.84, which indicates excellent agreement between the field data and the classification. Imagery from Franks Tract shows clear differences from 2004 to September 2015 and October 2016, which we attribute to the Barrier's effects (Figure 9). In 2004, the central section of Franks Tract remained mostly clear of SAV, which we attribute to tidal flow entering Franks Tract from the "nozzle" of False River (Figure 1). The northeast corner of Franks Tract, which gets a smaller influx from Old River (Figure 9A), also stayed clear of SAV. Five months after Barrier installation, (September 2015), SAV mats occupied the entire central section of Franks Tract, while SAV distribution was somewhat reduced from its earlier high coverage in the two openings on the northeast corner, likely because the strongest tidal flow during this period was through Old River (Figure 9B). By October 2016, 1 year after removal of the Barrier, the central section of Franks Tract appeared to be losing SAV (Figure 9B). Despite this initial clearing, SAV has stayed at its maximum extent even after the Barrier was removed (Figures 9C, 9D, and 10), and the central area of Franks Tract retained SAV at a low density even after high flows in early 2017.

Field data collected concurrently with image data in Franks Tract show a shift in species composition from an *Egeria densa*- and algae-dominated system in 2004 to a more mixed community dominated by sago (*Stuckenia pectinata*), Richardson's pondweed (*Potamogeton richardsonii*), *Egeria densa,* and coontail (*Ceratophyllum demersum*) in 2015 and 2016 (Ustin et al. 2016). With the Barrier in place in 2015, 90% of the SAV extent was Richardson's pondweed, while *Egeria* and coontail dominated at the edges of Franks Tract. Even the central area had been invaded, and the clear areas near the tidal inflows and outflows were few, narrow, and short. The Barrier may have helped SAV gain a foothold in Franks Tract where it had not been prevalent before. The SAV extent did not decline in 2016 and 2017, as seen in Figure 10 (red indicates presence of SAV).

The differences in extent cannot be unequivocally linked to the Barrier, given the increasing trend in SAV area in the Delta between 2004 and 2015 (Ustin et al. 2016) and the sensitivity of the freshwater SAV to salinity. However, the change in distribution patterns is likely a result of a change in flow patterns within Franks Tract. To

https://doi.org/10.15447/sfews.2019v17iss3art2

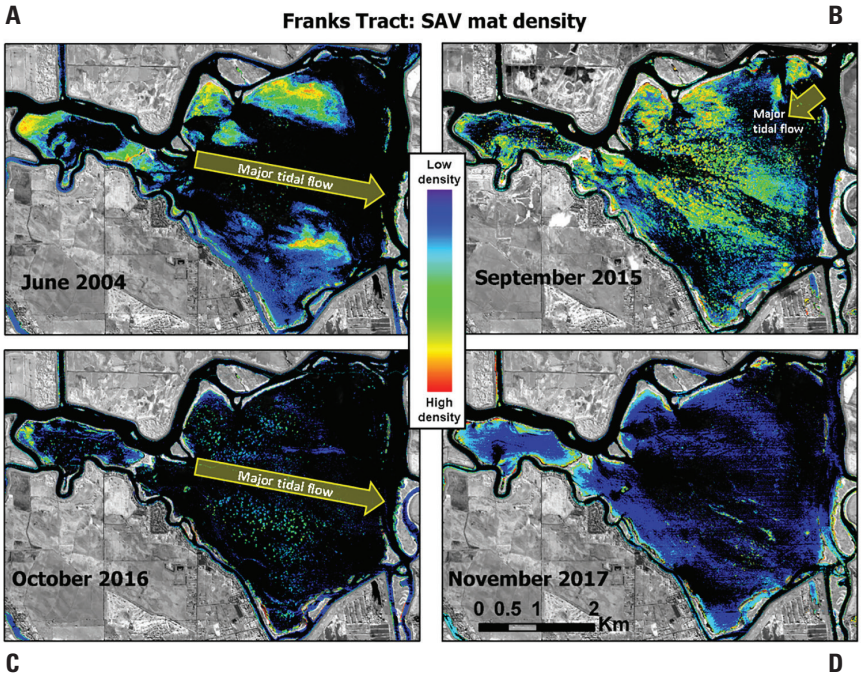

Figure 9 Density of submerged vegetation mats based on NDVI values in Franks Tract in (**A**) June 2004; (**B**) September 2015; (**C**) October 2016; and (**D**) November 2017.

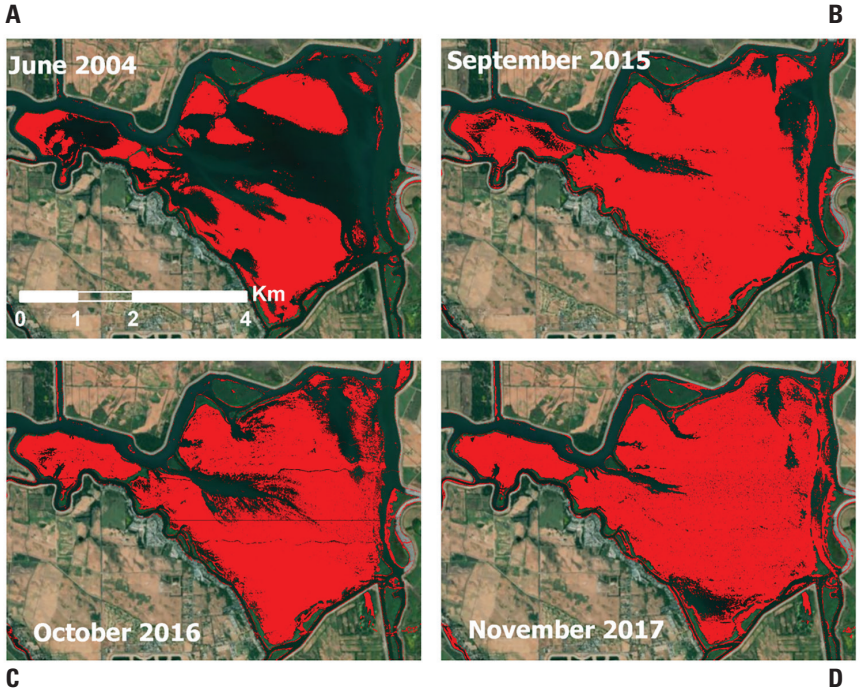

Figure 10 Extent of SAV (in red) in Franks Tract in (**A**) June 2004; (**B**) September 2015; (**C**) October 2016; and (**D**) November 2017.

further help separate the long-term pattern from any Barrier effect, we compared the distribution of SAV in Franks Tract to the distribution in Big Break (Figure 1B). Being seaward of Franks Tract, Big Break is exposed to higher salinity than Franks Tract. Moreover, hydrodynamic simulations during the Barrier's installation indicate increased salinity in Big Break during its period of operation. In Big Break, SAV mat density (and extent) increased from 2004 to 2015, but the general patterns of SAV mat distribution were similar in both years (Figures 11A and 11B). In 2016 (Figure 11C), these patterns did not change much, except for a slight decrease in the southern section of Big Break. In 2017, imagery was collected later in fall (November), hence the apparent clearing up of SAV might just indicate the onset of senescence. Thus, higher salinity did

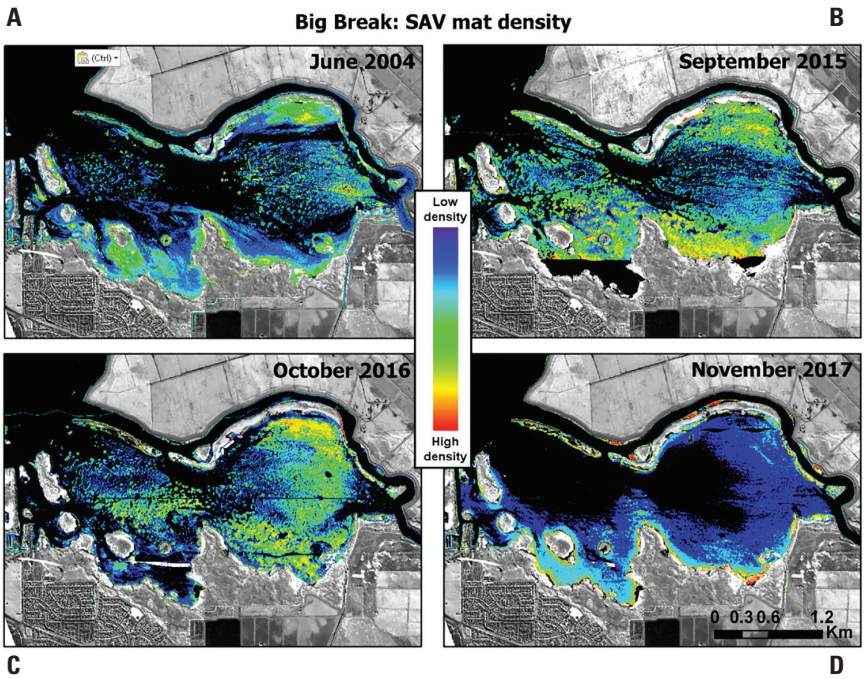

Figure 11 Density of submerged vegetation mats based on Normalized Difference Vegetation Index (NDVI) values in Big Break in (**A**) June 2004; (**B**) September 2015; (**C**) October 2016; and (**D**) November 2017

not result in lower SAV density; however, it does appear to have changed the SAV composition. Until 2015, Big Break supported a diverse SAV community, with more salt-tolerant species such as sago, curly-leaf, and American pondweed, in addition to some *Egeria* and coontail. By fall of 2017, another invasive species, *Cabomba caroliniana*, had gained a foothold in Big Break, spreading across large areas in monocultures (Ustin et al. 2016). As with Franks Tract, this change might not solely be because of the Barrier, but the Barrier might have helped more salt-tolerant species to establish, giving them a foothold in Big Break as a result of increased salinity.

WATER QUALITY AND WATER AGE

Low-flow conditions and placement of the Barrier were expected to influence water age as well as phytoplankton and nutrient concentrations (Table 1). To evaluate potential effects under with-Barrier and no-Barrier conditions, we used high-speed boat mapping to record the spatial distribution of water quality (WQ) and water age (τ) and assess potential changes (Appendix A; Downing et al. 2016). Previous research has shown that τ is a major driver of environmental and biogeochemical processes in the Delta, affecting trophic subsidies to the pelagic food web (Glibert et al. 2014; Dahm et al. 2016). In the Delta, τ is highly variable because of changes and patterns in fluvial and tidal hydrology, tidal wetlands, and changing landscape morphologies — engineered floodplains and simplified trapezoidal channels — all of which combine to affect τ in unpredictable ways (Durand 2015).

Results and Discussion

Maps of transect times and tide times are given for each date of the study (Figure 12). Water isotope values over the study ranged from −81.7‰ to −43.9‰ (δ^2H) and −12.1‰ to −5.4‰ (δ^{18}O), and are within ranges previously measured in the Delta (Kendall et al. 2015; Downing et al. 2016). Evaporation to inflow ratios (χ) ranged from 0.015 to 0.25, indicating that 1.5% to 25% of the inflowing water evaporated during the measurement periods (Skrzypek 2015; Downing et al. 2016; Appendix A).

All maps showed evaporative enrichment of water isotopes, and, accordingly, τ was usually highest south of Franks Tract and in the Old and Middle rivers, with or without the Barrier (Figure 13). With the Barrier in, τ was lowest (1 to 5 d) in the lower Mokelumne River, because the DCC

https://doi.org/10.15447/sfews.2019v17iss3art2

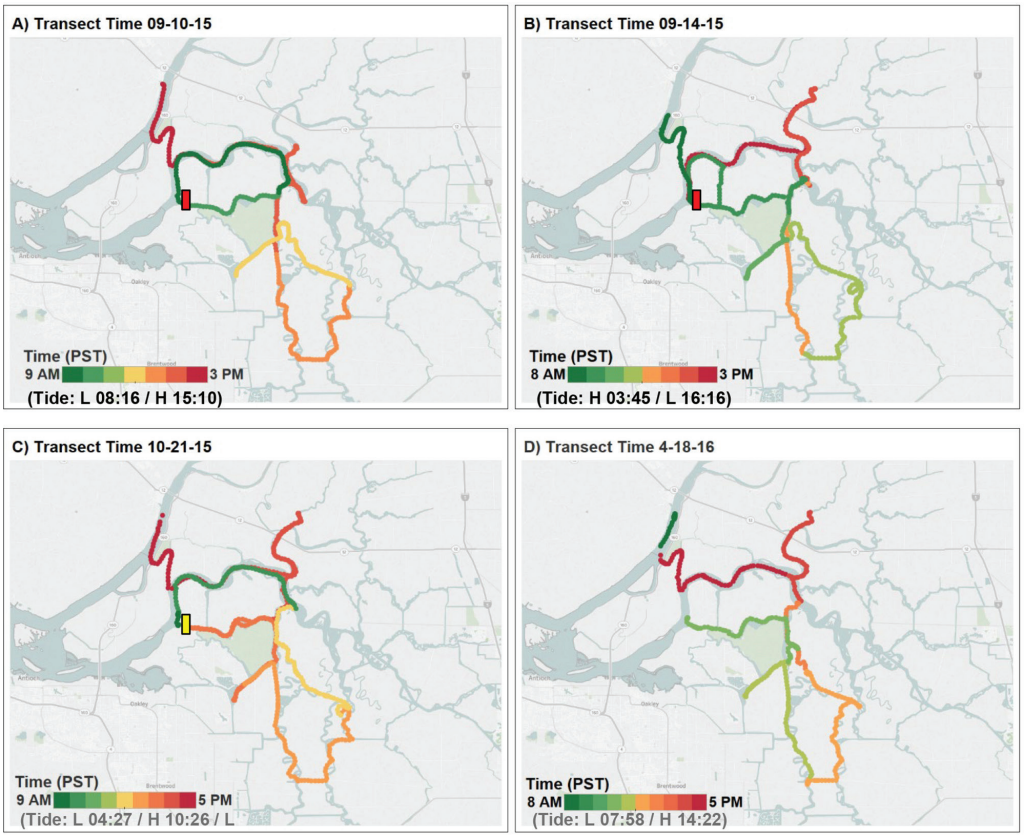

Figure 12 Maps of transect time (Pacific Standard Time; PST) for each date of study. Transects begin and end in the Sacramento River at Rio Vista, CA. *Color bars* show time of day in hours, where *steps of the color bar* show each hour of the transect from morning to evening. Tide times (PST) are shown *beneath the color bar*. Barrier is shown in *red* when fully in place (10 & 14 September 2015) and *yellow* (21 October 2015) when the Barrier was partially removed).

was open during September and October 2015 (Figure 13). Water quality in the lower Mokelumne River is often similar to that of the Sacramento River, since a fraction of the Sacramento River is diverted through the DCC into the Mokelumne River. In the channels that surround Franks Tract and in Threemile Slough, northwest of Franks Tract, τ was much more variable (10 to 20 d) as a result of differences in tidal phase and mixing of water parcels from the Old, Middle, San Joaquin, and Mokelumne rivers.

With the Barrier in, salinity ranged from 0.02 to 2.0, with higher salinities in the Sacramento River and Threemile Slough reflecting the presence of the Barrier and tidal exchange from Suisun Bay; these differences vanished with the Barrier's removal (Figure 14). Nitrate concentrations ranged from 2 to ~30 µmol L^{-1} in all four transects (Figure 15). With the Barrier in, nitrate concentrations were higher to the north and lower south of Franks Tract (Figure 15). After the Barrier was breached, nitrate increased south of Franks Tract (21 October 2015), and it was highest after the Barrier was fully removed (18 April 2016), probably reflecting higher τ and outflows, both of which likely influenced the spatial distribution.

Chlorophyll-*a* fluorescence (fCHLa) ranged from 2 to 6 µg L^{-1}, and was highest in the Old and Middle rivers, associated with higher τ and lower nitrate with the Barrier in, and was also elevated in the Mokelumne River on 14 September (Figure 16). fCHLa was lowest in October 2015. The April 2016 transect showed low concentrations in the Sacramento and Mokelumne rivers, with slightly higher fCHLa in the Old and Middle rivers and in channels around Franks Tract.

High-speed water-quality mapping demonstrated that the Barrier effectively kept high-conductivity or high-salinity water from entering the South Delta. The Barrier's effect on τ is unclear, since we measured persistently high τ in the South Delta with and without the Barrier. Further, we had posited that regions of the Delta with high τ might retain nutrients (e.g., nitrate) leading to increased phytoplankton productivity measured as in vivo chlorophyll-*a* fluorescence.

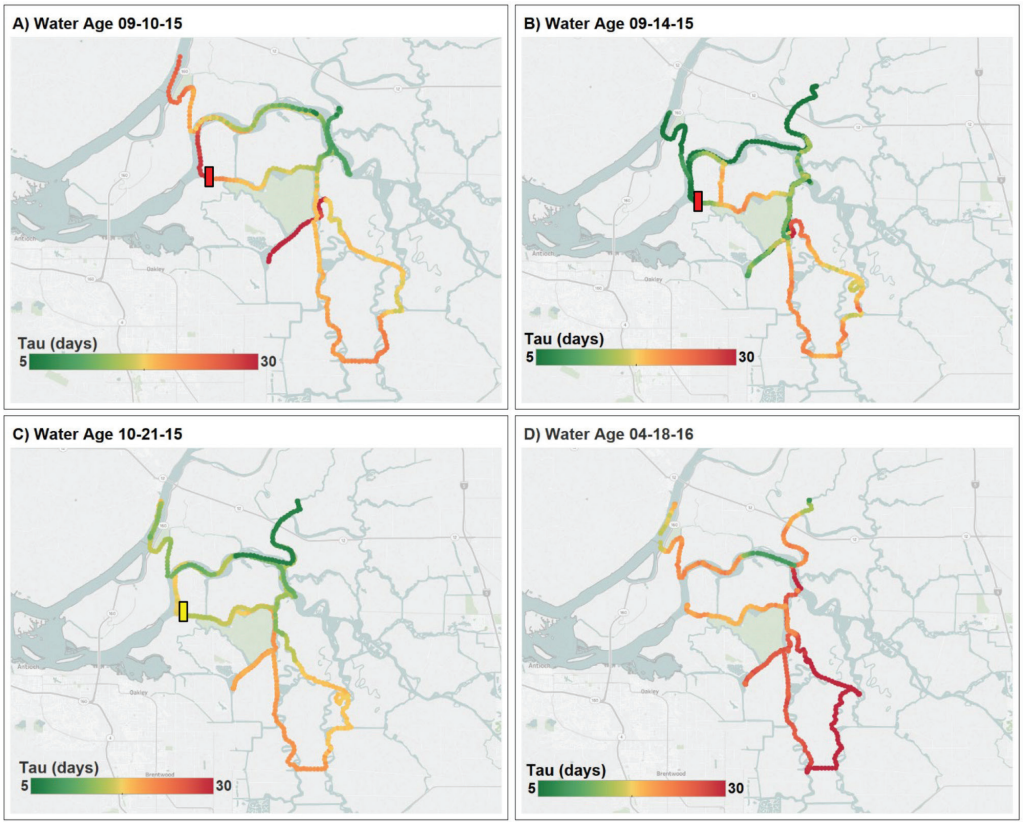

Figure 13 Maps of water age (τ; days) as in Figure 12

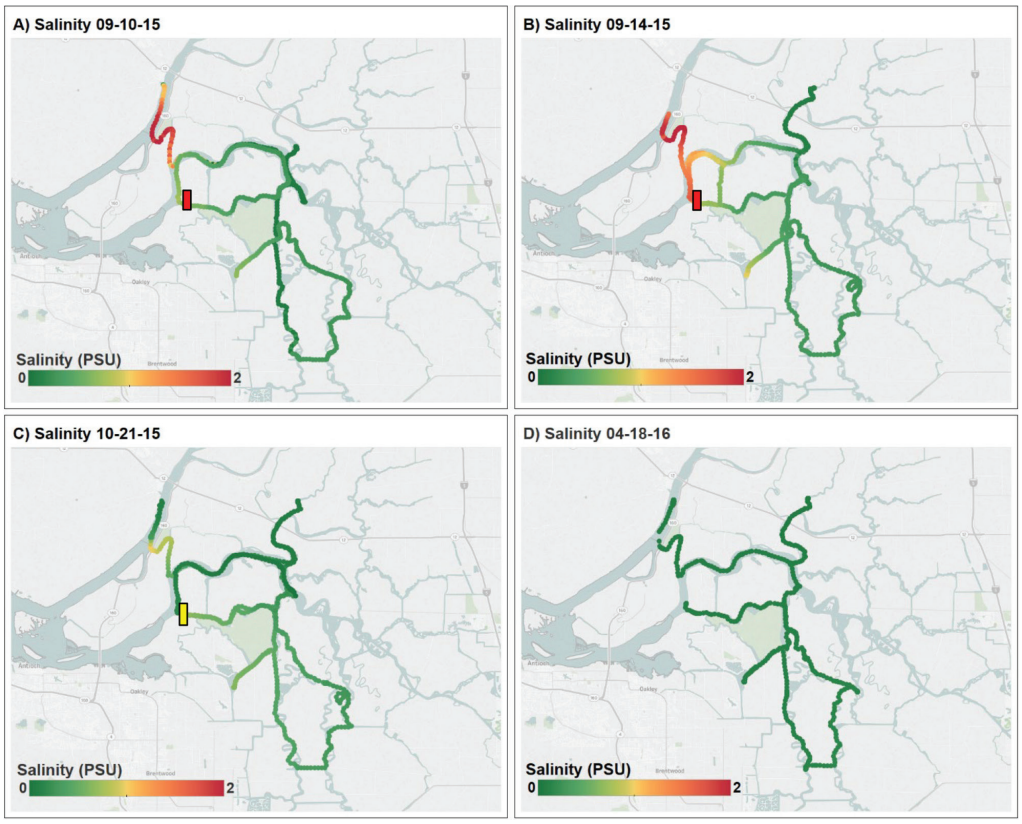

Figure 14 Maps of salinity (Practical Salinity Scale) as in Figure 12

https://doi.org/10.15447/sfews.2019v17iss3art2

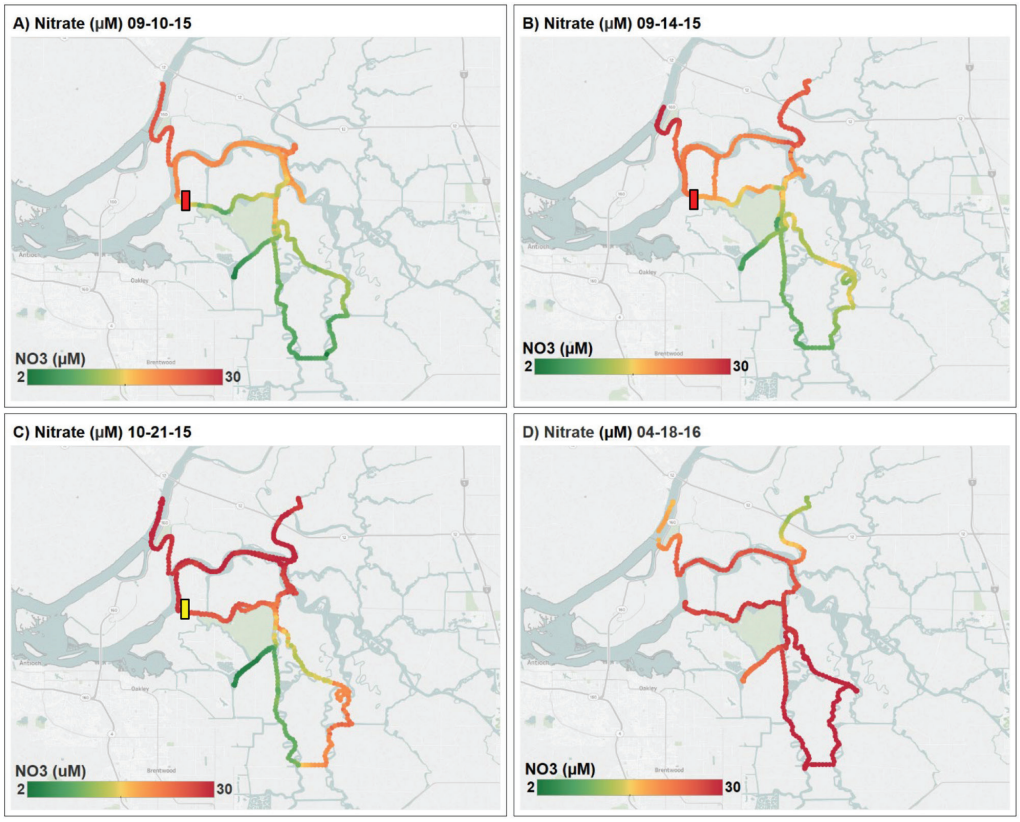

Figure 15 Maps of nitrate (µmol L^{-1}) as in Figure 12

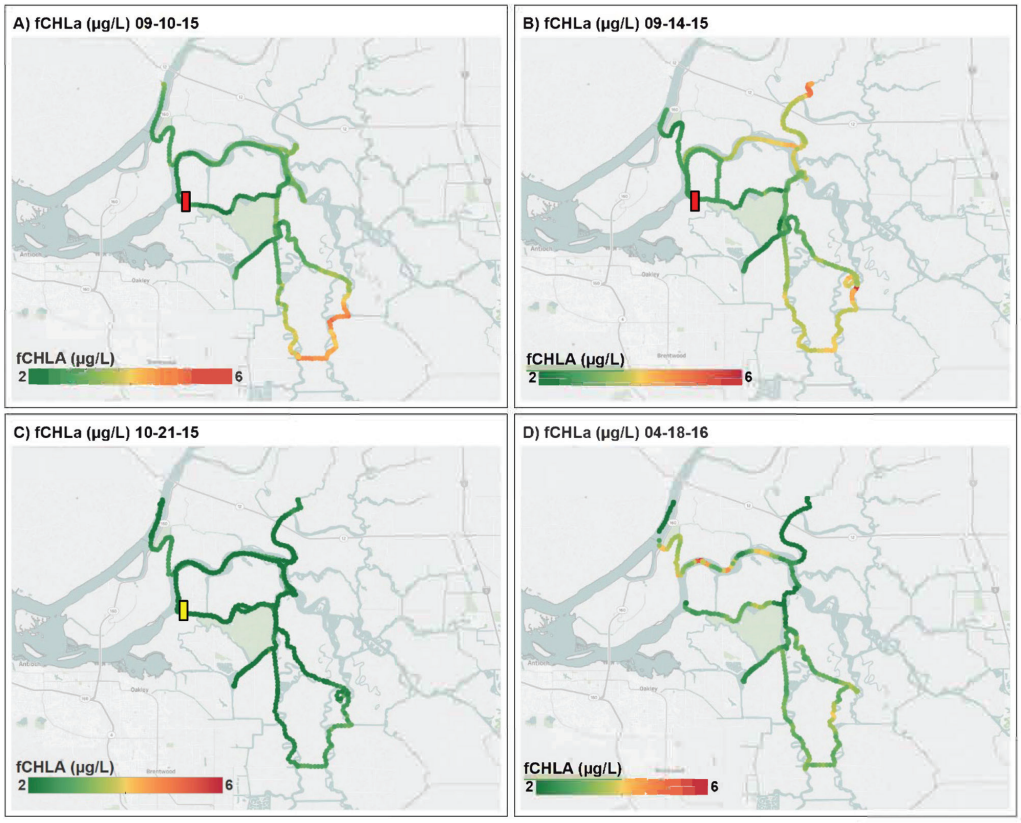

Figure 16 Maps of chlorophyll derived from fluorescence (µg L^{-1}) as in Figure 12

With the Barrier, we observed north–south gradients in nitrate and inverse gradients in chlorophyll-*a* fluorescence, implying net uptake of nitrate to produce phytoplankton in the South Delta. However, when the Barrier was removed and τ was again persistently high in the South Delta, we observed no increase in chlorophyll-*a* fluorescence (Figure 15).

NUTRIENTS AND PHYTOPLANKTON

Given the key role that phytoplankton play in the estuarine food web (Sobczak et al. 2005), as well as the summer–fall presence of the toxigenic cyanobacterium *Microcystis aeruginosa* in the Delta, any alteration of phytoplankton dynamics due to the Barrier would have important consequences for ecosystem function. This study element measured chlorophyll, nutrients, and *Microcystis* abundance at the intermediate to large scale, at 12 locations with and without the Barrier in place (Methods in Appendix A).

We anticipated that the Barrier's alterations of flow patterns could affect phytoplankton through decreased water flushing within and changes to the source water to Franks Tract, with increased influence of the nutrient-rich San Joaquin River (Table 1). Decreased flushing rate could result in increased water temperature and water clarity which, coupled with abundant nutrients, could result in increased chlorophyll accumulation (i.e., algal blooms) within Franks Tract. For example, *Microcystis* thrives in high temperatures (> 19 °C) and calm waters (Paerl and Huisman 2008; Lehman et al. 2013). Confounding the interpretation of possible Barrier effects were conditions associated with the drought in fall 2015, such as elevated nutrient concentrations (a result of lower dilution rate) and chlorophyll, as observed in the northern estuary in 2014 (Glibert et al. 2014). For this reason, our 2015 results were compared with results from prior drought years.

Results and Discussion

Our 2015 time-series (Figure 17) of surface chlorophyll concentrations in Franks Tract and station D15 (Figure 1A) showed no evidence of elevated chlorophyll with the Barrier compared to the no-Barrier condition (Figure 17A). The mean chlorophyll during both periods was ~4 µg L^{-1}, with larger cells (i.e., as represented by chlorophyll in cells > 5 µm) (Figure 17B) comprising 40% to 50% of the total. At D26, to the northeast of Franks Tract, there was increased chlorophyll (Figure 17A) that reached 6.9 µg L^{-1} after the Barrier was breached.

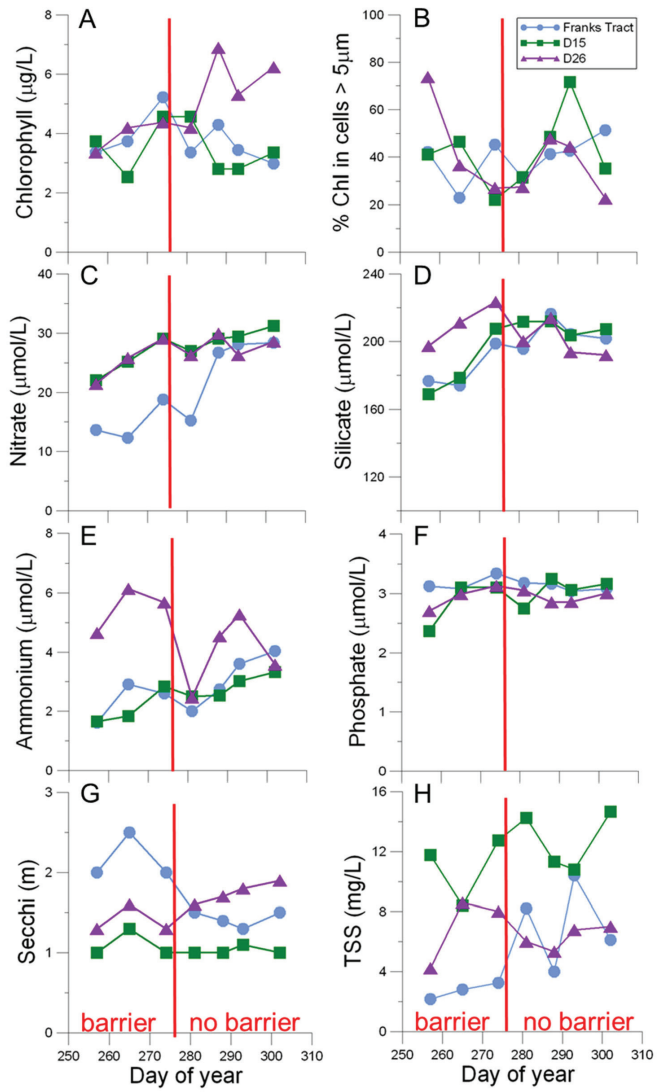

Figure 17 Fall (September to November) 2015 concentrations of: (**A**) chlorophyll (µg L^{-1}); (**B**) % chlorophyll in cells > 5 µm; (**C**) nitrate (µmol L^{-1}); (**D**) silicate (µmol L^{-1}); (**E**) ammonium (µmol L^{-1}); (**F**) phosphate (µmol L^{-1}); (**G**) Secchi (m); (**H**) TSS (mg L^{-1}) at Franks Tract (*blue*), D15 seaward (*green*), and D26 landward in San Joaquin River (purple; Figure 1). The red line shows the time of the breach.

https://doi.org/10.15447/sfews.2019v17iss3art2

At Franks Tract, nitrate, silicate, and ammonium concentrations and total suspended solids (TSS) had positive trends, and Secchi depth had a negative trend over the duration of the study (Figures 17C through 17H). Lower nitrate in September was also observed in the Water Quality and Water Age section (Figure 15; Appendix C). Similar, but smaller changes in these constituents were observed over the fall at D15. At D26, there was less water clarity and more TSS with the Barrier in place. We cannot determine whether these trends were a result of the Barrier, though a plausible mechanism is that the differences in TSS and water clarity between Franks Tract and the other stations with the Barrier in place arose because of reduced circulation (see "Movement of Water and Particles") and increased SAV coverage of Franks Tract (see "Submerged Aquatic Vegetation"). Reduced circulation would have reduced flushing, allowing more time for nutrient uptake by SAV, and reduced turbulent energy due to SAV would have allowed particles to settle from the water column, decreasing TSS and increasing water clarity. The changes in Franks Tract following the breach may also have been accelerated by the seasonal die-back of SAV.

The abundance index of *Microcystis* colonies in surface water (Figure 18) showed the cyanobacteria to be present throughout the study area, and slightly more abundant at landward locations (i.e., Franks Tract and San Joaquin stations D26, L14, and L34). *Microcystis* did not reach the high levels observed at these locations in 2011 and 2012 by Lee et al. (2015) using the same index, even though water temperatures were > 19 °C throughout our study period. The patterns were generally similar between with-Barrier and no-Barrier conditions.

To evaluate whether changes seen in the fall 2015 time series (Figure 17) may be attributed to the Barrier and breach of the Barrier, or be seasonal changes that occur during drought conditions, we compared our fall 2015 data for Franks Tract and D26 with monthly monitoring data from other drought years (2008–2010, 2012, 2014–2016) collected by IEP (Figure 19), although these data were collected from 1 m depth, compared to our surface samples. The Franks Tract data (Figures 19A, 19C, 19E, and 19G) support the conclusion that the Barrier had a negligible effect on chlorophyll and most nutrients, because the time series in fall 2015 resembled those in other dry years, showing similar levels of chlorophyll and increasing nutrient concentrations as fall progressed. Chlorophyll in most years (including 2015) did not reach the high levels of 8.5 and 10 µg L^{-1} that Lee et al. (2015) observed at Franks Tract during *Microcystis* blooms in 2011 and 2012. At Franks Tract, during September (days 250 to 274), TSS values were the lowest during the with-Barrier condition, and then, after the breach, values were similar to other dry year data.

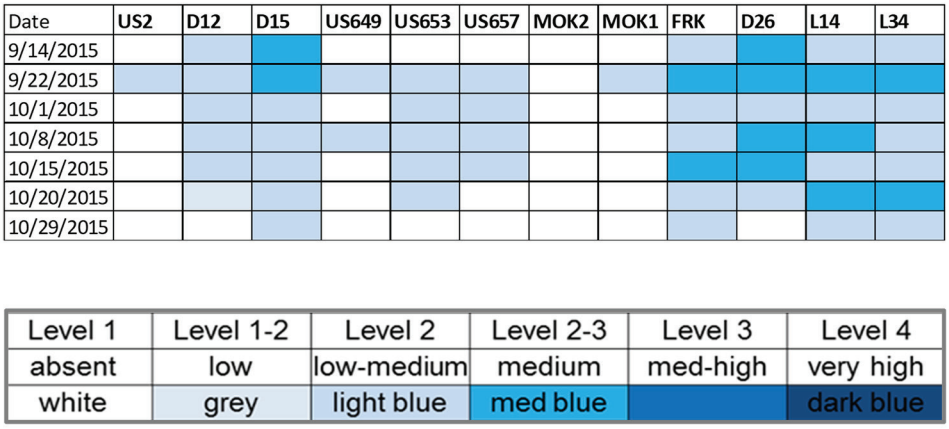

Figure 18 Heat map showing relative abundance of *Microcystis* colonies in surface water observed during fall 2015 at locations shown in Figure 1

In contrast, in 2015 at D26 in the San Joaquin River northeast of Franks Tract, chlorophyll and nitrate were higher than in previous years (Figures 19B and 19D). This was not the case for ammonium or TSS concentrations (Figures 19F and 19H). Elevated chlorophyll was also observed in 2015 in that region, at the Mokelumne River (MOK 1) location (Figure 1; Appendix D), with concentrations ranging from 7 to 27 µg L^{-1}, higher than previously observed at this location in summer–fall 2011 and 2012, when chlorophyll did not exceed 2 µg L^{-1}. The higher tidal flow in the region near the Mokelumne and D26 (Figure 4) with the Barrier may have delivered more nutrients and stimulated higher chlorophyll; then, with removal of the Barrier, the reduced flow may have aided chlorophyll accumulation.

We further compared 2015 data (from IEP and this study) with mean data collected in fall during different water years officially categorized as critically dry (2008, 2014); dry or below normal (2005, 2007, 2009, 2010, 2012, 2013, 2016); and wet (2006, 2011) (*http://cdec.water.ca.gov/reportapp/javareports?name=WSIHIST*). Data for each water-year type were averaged (with dispersion presented as 95% confidence limits; Figure 20). This synthesis supports the observations above that at Franks Tract there was no detectable difference in chlorophyll, nutrients, or TSS in the fall 2015 data (collected during both with-Barrier and no-Barrier conditions), compared to data from other critically dry years with no Barrier (Figure 20). However, nitrate concentrations at D26 were higher than during other conditions, including critically dry, indicating that the Barrier may have affected nitrate at D26. The wide 95% confidence limits for the mean chlorophyll data from 2015 are likely the result of combining our surface data with the 1-m-depth IEP data, and for the critically dry condition by the very high and low values measured in 2014 by IEP. Other mean nutrient concentrations did not vary appreciably with flow conditions.

In summary, anticipated phytoplankton blooms at Franks Tract did not occur, although water clarity was greater and TSS lower with the Barrier. Although the 2015 time series suggested that changes in nutrients at Franks Tract might be associated with the Barrier, these changes were also observed seasonally in other dry and critically dry years. Finally, at D26, northeast of Franks Tract, there were elevated chlorophyll and nitrate concentrations in fall 2015 that were higher than in other dry years, which suggests a possible link to the Barrier.

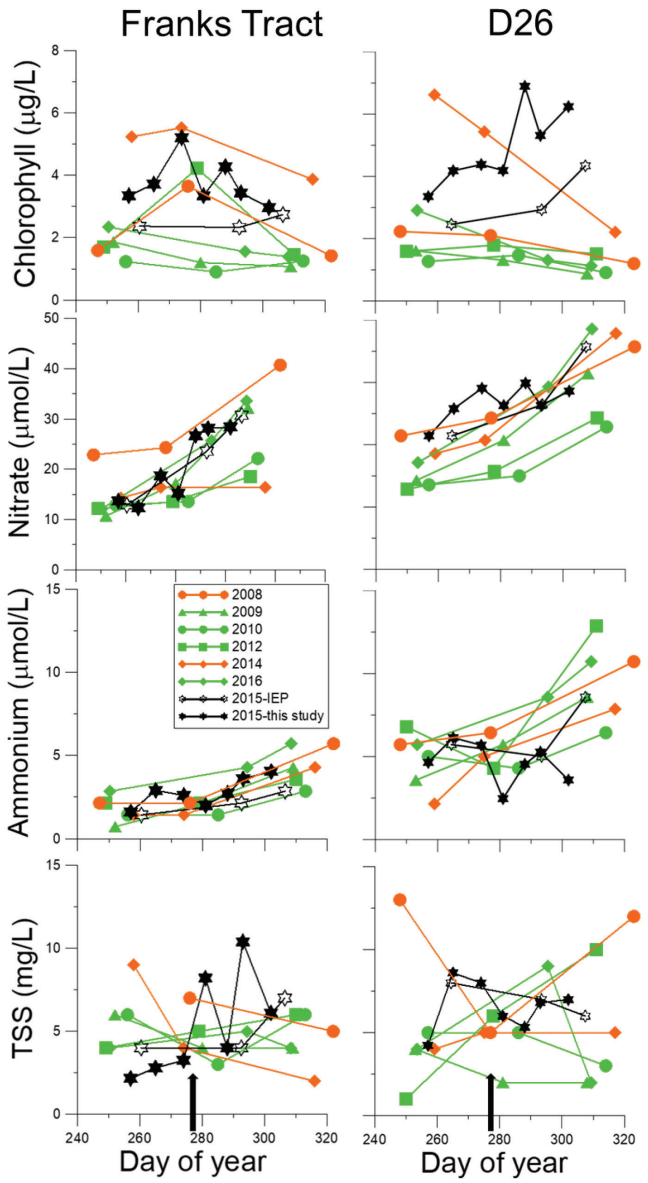

Figure 19 Fall (September to November) 2015 concentrations of (**A**, **B**) chlorophyll (µg L^{-1}); (**C**, **D**) nitrate (µmol L^{-1}); (**E**, **F**) ammonium (µmol L^{-1}); (**G**, **H**) total suspended solids (TSS) (mg L^{-1}) at Franks Tract (*left*) or D26 (*right*) during dry years from 2008 to 2015 (critically dry: *orange*, dry: *green*, 2015: *black*); *black arrow* shows time of barrier breach in 2015.

https://doi.org/10.15447/sfews.2019v17iss3art2

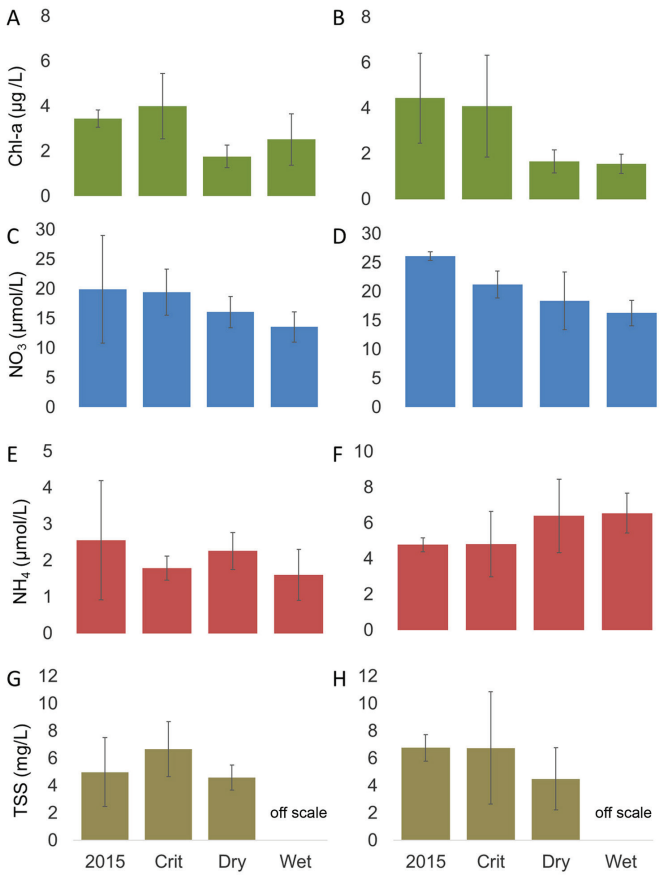

Figure 20 Mean (± 95% confidence intervals) concentrations of (**A**, **B**) chlorophyll (µg L^{-1}); (**C**, **D**) nitrate (µmol L^{-1}); (**E**, **F**) ammonium (µmol L^{-1}); (**G**, **H**) TSS (mg L^{-1}) at Franks Tract (*left*) or D26 (*right*). Note different y-axis scales for two locations. Data are means for fall (September to November) 2015 (this study and from IEP) and from IEP data for critically dry (2008, 2014), dry and below normal (2007, 2009, 2010, 2012, 2012, 2016), and wet (2006, 2011) years. Note: TSS during wet years was excluded because the values exceeded TSS under other water year types by several fold.

BIVALVES

Two exotic filter-feeding bivalves, *Potamocorbula amurensis* and *Corbicula fluminea*, have been reported to control phytoplankton biomass in the estuary, including the Delta (Lopez et al. 2006). Distributions of the recruits of these bivalves overlap at a salinity of about 2, while the adults are much more tolerant of salinity change and can overlap anywhere between freshwater and a salinity of 10 (Hartman et al. 2017). Therefore, we expected both species to occupy the area in the vicinity of the Barrier affected by the changes in salinity that resulted from the Barrier (Table 1). We examined the distribution of each bivalve species before, during, and after the Barrier was in place. We expected that the Barrier's purpose — to limit the penetration of salt into the South-Central Delta — would result in saline waters and therefore *Potamocorbula* moving into the confluence and further up the San Joaquin and Sacramento rivers.

Grazing capabilities also differ between these species. *Potamocorbula* has a biomass-specific pumping rate about four times that of *Corbicula*, and therefore a *Potamocorbula* population will result in a larger grazing rate and phytoplankton loss rate than a *Corbicula* population of the same biomass. *Potamocorbula* can consume copepod nauplii (Kimmerer et al. 1994; Kimmerer and Lougee 2015) and therefore can directly affect the abundance of both phytoplankton and zooplankton.

Bivalve biomass, shell length, grazing rate, and recruitment data (see Methods in Appendix A) were available in May and October 2007–2015 from CDWR (2019 email from B. Wells to WK, unreferenced, see "Notes"). These data gave us valuable context for the period before the Barrier's placement. We examined these data, in addition to new samples in August, September, and November 2015 as well as January, June, and October 2016 for each bivalve species in the geographic regions we expected to be most influenced by changes in salinity due to the Barrier: the confluence and western San Joaquin River (between Franks Tract and New York Slough; Figure 1B), and southwestern Sacramento River (between the upper end of Decker Island and New York Slough; Figure 1B).

Results and Discussion

Reflecting the seasonal penetration of salinity into the western Delta in dry summers-falls, *Corbicula* biomass persistently dominated in the rivers (San Joaquin River West [SJR West] and Sacramento River South [SR South]) before 2015, and *Potamocorbula* biomass was often dominant in the confluence throughout 2007–2016 (Figure 21A). *Corbicula* biomass was somewhat higher in spring than fall, and *Potamocorbula*

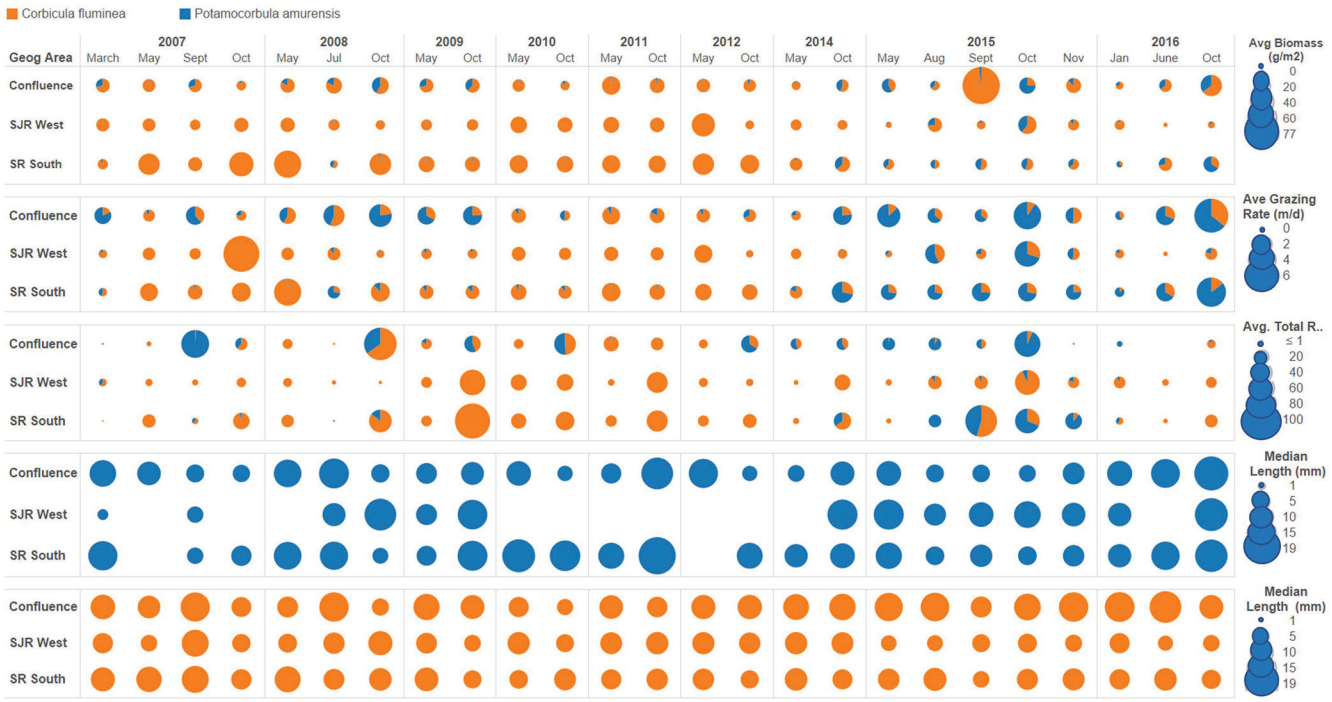

Figure 21 (**A**) Mean biomass; (**B**) grazing rate: (**C**) number of recruits; and (**D**) median length of *Corbicula* and (**E**) *Potamocorbula* within three geographic areas for the 7 years prior, 1 year during, and 1 year after the Barrier was in place.

biomass seasonality was the opposite. *Potamocorbula* intruded into the confluence and SR South regions as salinity increased upriver during dry years (2008–2009, 2012–2015); *Potamocorbula* biomass was highest in these regions in October 2014 through January 2016. *Potamocorbula* appeared in SJR West in 2015 after the Barrier was constructed, and persisted at lower biomass levels through 2016 after the Barrier was removed.

Grazing rate data highlight the importance of the presence of *Potamocorbula* in the confluence and SR South regions (Figure 21B). *Potamocorbula* grazing rate increased in the confluence relative to *Corbicula* grazing rate in 2014 and 2015, and was already important in that region when the Barrier was built. In the confluence, where the depth (z) is about 3 m, grazing turnover times (z/GR) were 4 to 7 d, indicating that the two bivalves together likely influenced accumulation of phytoplankton biomass (Lucas and Thompson 2012). Over the multi-year dry period when *Corbicula* biomass and grazing rate declined, biomass and the grazing rate of immigrating *Potamocorbula* exceeded losses from *Corbicula* (Figures 21A and 21B).

As expected, recruits from both species were common in the confluence region, and *Corbicula* recruits dominated in both rivers (Figure 21C). We saw higher *Potamocorbula* recruit abundance in the confluence during Barrier construction in May 2015 than in springs of other years; *Potamocorbula* recruits usually settle in fall in the confluence (Figure 21C). *Potamocorbula* recruits were unusually abundant in the confluence in October 2015. In addition, *Potamocorbula* recruits were previously uncommon in the rivers, but were relatively abundant in SR South and present in SJR West from August 2015 through January 2016 (Figure 21C). *Corbicula* recruits were mostly limited to SJR West and SR South, where recruit abundance was lowest during the Barrier period in May 2015 through January 2016. In all cases, the distribution of recruits was consistent with the salinity distribution (Figure 3).

Maximum length and age of *Corbicula* (50 mm, 5 years) is much greater than that of

https://doi.org/10.15447/sfews.2019v17iss3art2

Potamocorbula (25 mm, 2.5 years). Therefore *Corbicula* populations can survive more years of higher salinity and low recruitment than *Potamocorbula* populations can withstand multiple years of exposure to freshwater. As a result the median size of the animals, and therefore tolerance to a range of salinities, is much less dynamic for *Corbicula* than for *Potamocorbula*. The stable, elevated salinity near the Barrier allowed adult *Potamocorbula* to grow to a sufficient size that they were apparently resistant to the salinities seen in 2016 that were limiting to their recruits (Figures 21D and 21E). Median size of *Potamocorbula* usually decreases as the recruit numbers increase, but in January 2016 the median size of *Potamocorbula* increased coincident with declines in salinity and declines in abundance of recruits.

The broader salinity range of adults than of recruits of both species allows adults to occupy locations at the edges of their salinity tolerance. In those years when both spring and fall salinity were high enough for *Potamocorbula* recruits to settle, as in 2014 and 2015 in the confluence (Figure 21C), the spring recruits grew sufficiently to withstand the subsequent fall-winter freshening of the Delta. Thus, the effects of *Potamocorbula's* movement upstream extended into the next year, with the larger animals being present at the landward edge of their habitat in the subsequent spring, as occurred in 2012 and 2016 in the confluence. Similarly, *Corbicula* can persist in regions where salinity is too high for recruitment (e.g., confluence, May 2015; Figures 21A and 21C).

Both bivalve species recruit and grow at the edges of their salinity tolerance, which constantly changes position in this estuary. Because *Corbicula's* lifespan is twice that of *Potamocorbula* they can persist longer at downstream habitat edges, and they are therefore present in the confluence during most years. *Potamocorbula* has its largest effect in the confluence during successive dry years when the adults can reproduce in a dry spring, and the larvae are transported and survive further upriver, thereby extending their distribution upstream into the Sacramento River as salinity increases. The result of this immigration, as seen in our example in 2015, is higher grazing rates that may persist across multiple years when low salinity would otherwise be expected to limit their distribution.

As expected, the distribution of the two bivalve species after the Barrier's placement reflected the salinity distribution. However, since the adult populations of both species can remain after salinity returns to levels that would challenge recruits, what appear as short-term changes are likely to be much longer-term. The duration of the resulting population distributions may reflect the lifespan of each species, particularly if the years after salinity is altered are years of mean or higher freshwater runoff. The altered distribution of the bivalves likely affected the food web through higher grazing rates during the presence of the Barrier. But for the 1-year period observed in this study, the post-barrier grazing rates were similar to those seen in prior years.

SYNTHESIS

We used a weight-of-evidence approach that combined (1) modeling with well-calibrated hydrodynamic models, (2) examination of observational evidence for consistency with a Barrier effect, and (3) consideration of plausible mechanisms to assess Barrier effects. Despite differences in study design, sampling locations, and reference periods among study elements, we were able to conclude that the effects of the Barrier were either as expected (hydrodynamics, SAV, bivalves) or smaller than expected (nutrients, phytoplankton, zooplankton).

None of the analyses showed substantial responses at the large scale (Figures 1A and 1B). Most analyses focused on the intermediate scale (in and near Franks Tract, Figure 1B); for example, the SAV analysis found effects at that scale, as expected. The zooplankton analysis found evidence of an effect on transport only at the intermediate scale, and no apparent effect on abundance at the larger scale. The phytoplankton and nutrient data showed little evidence for effects at the intermediate scale.

Later we discuss effects of the Barrier that have strong support and others without such strong support. We did not include several topics in the suite of studies reported here. Presumably, the Barrier altered the movements of fish, and the outcomes of this effect could be investigated using available survey data, although at current low abundances Barrier effects may have been difficult to detect. Also, we did not investigate contaminant effects. Finally, we did not consider physical effects that resulted from alterations of flow patterns in the Delta, such as scouring and sediment deposition, which have been adequately addressed elsewhere (CDWR 2017).

Observed and Inferred Effects

The hydrodynamic influences of the Barrier are readily apparent, since the purpose of the Barrier was to alter intermediate-scale water movement, and because hydrodynamic models demonstrate these effects unambiguously (e.g., Figure 4). The Barrier eliminated tidal flows that entered Franks Tract from the San Joaquin River via False River, and increased tidal flows into Franks Tract from Fisherman's Cut and from the northeast (ORFT, Figure 1). Hydrodynamic effects beyond the intermediate scale appeared to be negligible (Table 4), and high-speed mapping did not show variability in water age that could be attributed to the Barrier. The Barrier kept salinity in the Old River south of Franks Tract at the same low level as in 2014, despite higher salinity in the San Joaquin River at Jersey Point (Figure 3).

Earlier imagery (Figures 9A and 10A) and the accessibility of central Franks Tract by boat in summers without a barrier indicate a persistent vegetation-free channel across Franks Tract. It presumably resulted from strong tidal currents coming from the False River "nozzle" (Figure 1B). With the Barrier in place and no "nozzle," SAV colonized all of Franks Tract (Figure 10), and the formerly clear region became inaccessible by boat. This speaks to the spatial extent of the SAV but not whether the per-area biomass of SAV increased. SAV colonization may have delayed re-establishment of tidal currents within Franks Tract even after the Barrier was breached, but we lack time–series data to determine this. Recent classification from November 2017 imagery (Figure 10D) seems to support depressed tidal currents in vegetated regions because Franks Tract still showed almost 100% cover by SAV. The lag in recovery of the daily salinity range in Franks Tract after the breach (Figure 3) is likely a result of weak salinity gradients in this region of the estuary, and may have influenced, and been influenced by, the distribution of SAV. Hydrodynamic modeling did not include the effect of SAV on reducing water flow.

The distributions of bivalves appeared to respond mainly to salinity (Figures 3 and 21), which can be interpreted as a combination of a drought effect and a Barrier effect. Young bivalves settled in regions of suitable salinity that were more defined than the regions where adults occurred (Figure 21C). Interannual persistence of adult bivalves at salinities where juveniles cannot settle (either too high for *Corbicula* or too low for *Potamocorbula*) results in substantial spatial overlap between the two species, and a lack of strong salinity response in community grazing rate. However, the higher grazing rate per unit biomass of *Potamocorbula* can result in higher total grazing rate if salinity remains high long enough (months) so that settled *Potamocorbula* can resist subsequent freshening.

Some ephemeral effects of Barrier construction and removal were anticipated and observed. This included a reduction in water clarity and elevation of TSS at Franks Tract after the Barrier was breached (Figures 17G, 17H, 19G, and 19H), presumably a result of re-suspension of sediment that had settled near the Barrier because of reduced local-scale current speeds (Figure 4).

Changes Anticipated but Not Observed

Neither high-speed mapping nor repeated sampling showed an intermediate-scale effect of the Barrier on nutrient concentrations or phytoplankton biomass (Figures 15, 16, and 17). The lack of response of phytoplankton in October may have been due to grazing by clams, which probably exceeded phytoplankton growth rate (Figure 21; Kimmerer and Thompson 2014). Chlorophyll concentration was elevated in the Mokelumne River (Figure 16; Appendix D) and in the San Joaquin at D26 (Figure 17A) to the

https://doi.org/10.15447/sfews.2019v17iss3art2

northeast of Franks Tract, as shown by both mapping and nutrient measurements; however, this cannot be linked unequivocally to the Barrier or its effect on tidal flows, because of the lack of an intermediate-scale effect or a plausible mechanism for an effect that reached past the intermediate scale into the Mokelumne. In addition, the often-unpredictable outbreak of phytoplankton blooms in the estuary (e.g., Dugdale et al. 2012) suggests caution in assigning a particular cause to an isolated instance of high biomass.

One concern was that reduced flow in Franks Tract might favor blooms of toxigenic *Microcystis* which have occurred there (e.g., Lehman et al. 2008). However, this slow-growing cyanobacterium was no more abundant during 2015 (Figure 18) than in other dry years, so if the Barrier had an effect it was offset by other factors.

Exchange modeling coupled with patterns of copepod abundance showed that the Barrier likely reduced the transport of copepods from fresh toward brackish water at the intermediate scale (Figure 7), but distributions of copepods at the larger scale (Figure 8) did not reflect this reduced transport. Thus, based on our analyses, the Barrier had little effect on the supply of food to Delta Smelt. Copepod abundance at a particular location is a result of cumulative processes of birth, development, death, and movement. All of these processes vary spatially and temporally, and none can be measured very precisely (Kimmerer et al. 2014, 2017, 2019). Tidal mixing across abundance gradients mediates a large part of plankton movement in dry periods when net flows are small, so the most suitable method for estimating movement is through modeling, as done here. The values in our exchange matrix (Table 4) are likely accurate; though the data used to determine abundance gradients in the box model are highly variable, the conclusion of a small, but ecologically unimportant Barrier effect on transport seems robust.

It is possible that interactions occurred but were not detected in the data. For example, we would expect that the redistribution of bivalves should have affected spatial patterns of both chlorophyll concentrations and copepod abundance. However, detecting such effects takes many observations over a period of time because of the high spatial and temporal variability of the bivalve populations and tidal and seasonal movement of phytoplankton and zooplankton with the salinity field (Kimmerer and Thompson 2014; Kimmerer et al. 2019).

Longer-Term Effects

Spring of 2016 was moderately wet: monthly mean X2 was seaward of the Delta during February to May, and most of the Delta was fresh. This freshening probably reset some conditions in the Delta that may have arisen during the previous years of drought, including the effects of the Barrier. SAV buildup and sediment deposition respond to flow conditions and may have been partially reversed during 2016 or during the very wet water year 2017, although SAV coverage persisted at least into 2017. Bivalve distributions can also be persistent once established, so the system may carry "memory" of the landward shift in recruitment patterns seen during the drought and Barrier operation (Figure 21).

Droughts of similar or greater magnitude to that of 2012–2015 are likely to become more frequent as increasing temperature reduces snowpack and shifts the runoff peak earlier (Roos 1989; Stewart et al. 2005; Berg and Hall 2017; Luo et al. 2017). Future use of drought barriers in the Delta therefore seems likely (CDWR 2018), unless the physical configuration of Franks Tract can be altered permanently to limit salt intrusion without the use of a barrier (CNRA 2016; CDFW 2018).

Would repeated or prolonged operation of a False River barrier, either temporary or in some more permanent form, have a cumulative effect on the ecosystem? Clearly, we can answer that only through speculation based on our partial understanding of the estuarine ecosystem and the knowledge acquired during this study. In particular, it is possible that longer-term operation of a barrier would induce cumulative, larger-scale effects that we did not observe. Moreover, we cannot forecast what interactive effects might occur with a future barrier, such as through alteration of ecological processes sensitive to temperature extremes or prolonged droughts or

major floods, or the introduction of more non-indigenous species (e.g., quagga mussel).

We anticipate that the most prominent effects of longer-term barrier operations would be in the distributions of organisms that shift spatially through reproduction and subsequently occupy physical habitat outside of their current range. Thus, SAV and bivalves may respond to barrier construction through increased colonization and occupation of habitat from which they are excluded by conditions without a barrier. Current speeds and salinity seem to be the factors that exclude SAV from some areas of Franks Tract and other parts of the Delta. Salinity appears to be the factor that controls the zone of overlap of the two bivalve species, although the relative importance of the Barrier in this control is uncertain. The location of this zone is important because of the 4-fold higher filtering rate per unit biomass of *Potamocorbula* than *Corbicula*. A future barrier will be most conducive to *Potamocorbula* expansion and an increase in grazing rate when the prior year is dry enough to allow spring recruitment and the persistence of adults until the next year. *Corbicula* recruit abundance will decline in the bivalve overlap areas because of the higher salinity, but the adults may remain in the area for several years. This makes clear that the effects of future barriers must be considered in the context of previous hydrology, and also that these effects are likely to carry into the future if the drought-with-barrier condition is followed by similarly dry conditions.

RECOMMENDATIONS FOR FUTURE BARRIER OPERATIONS

The estuary in general, and the Delta in particular, are highly modified systems in which natural processes have been altered through changes in factors such as tidal prism, extent of the wetted area, connectivity among sites and regions, and numerous introduced species including most of the species discussed here (much of the SAV, both bivalves, and the copepods). Given this backdrop, large-scale manipulations of the physical system to achieve societal benefits (in this case, keeping salt out of water supplies at minimal cost in stored water) should continue to be considered, with appropriate caution and analysis to show that they do not substantially degrade the system. Our results suggest that alterations to the estuarine ecosystem resulting from barrier operation were rather localized and probably ephemeral, though SAV and bivalves may be important exceptions. However, we had limited opportunities to compare the with-barrier to no-barrier conditions, and could not determine the carry-over effects of dry years following years of barrier operation. Nevertheless, if used with caution, these results provide a guide to future barrier operations.

Significant alterations to the configuration of the estuary should be made in an experimental framework to resolve high uncertainty about their effects. This calls for modeling of the effects of repeated barrier operations under different conditions such as various sequences of drought and high flow. It also calls for programs to gather reference data during dry years for comparisons with subsequent dry years when barriers are operated. For some responses (e.g., bivalves, SAV) samples can be gathered, stored, and subsequently analyzed only if needed for reference to with-barrier conditions.

The principal foci of a research program should be on the most likely effects (e.g., on circulation patterns, SAV, and bivalves) and on effects that could have important consequences, such as any effect on the prevalence of *Microcystis* blooms, but the program should also maintain the flexibility needed to respond to events and new information. The program should maintain a long-term perspective, examining results for evidence of cumulative effects, e.g., alteration of channel dimensions through scouring and deposition, with consequent effects on the ecosystem. Moored sensors designed to gather data on important barrier effects (e.g., current speed, SAV cover, turbidity, chlorophyll, *Microcystis*) could be prepared for deployment during dry periods with and without barriers in place. High-speed mapping could provide a spatial framework for the data from moored sensors, and alert researchers to changes that bear investigation.

https://doi.org/10.15447/sfews.2019v17iss3art2

Finally, it is useful to remember that the estuary ecosystem is in a state of continual change. Any action taken to improve water supply should also consider effects on the ecosystem, and vice versa. Thus, future decisions about installing temporary or operable barriers should be made with a long-term perspective.

ACKNOWLEDGEMENTS

Funding for the original projects was provided under Delta Science Program Grant Agreements 2283 to USGS (BD) and 2284 (WK and EG) and 2286 (RD, FW, and AP) to San Francisco State University; and NASA Grant NNX14AD79G to Oregon State University with subcontract to SFSU (RD). Synthesis contracts were provided by Delta Science Program Grant Agreements 5016 (WK), 5017 (FW), 5018 (EG), 5019 (AP), 5021 (RD). We thank the many people who helped during field work including Edmund Antell, David Bell, Sarah Blaser, Erica De Parsia, Sharon Gosselink, Angela Hansen, Ann Holmes, Jamie Lee, Tricia Lee, David Morgan, Kyle Nakatsuka, Katy O'Donnell, Francis Parchaso, Sarah Pearson, Anne Slaughter, Elizabeth Stumpner, and Travis von Dessonneck. Steve Andrews worked with EG on the hydrodynamic and particle-tracking modeling.

REFERENCES

Andrews SW, Gross ES, Hutton PH. 2017. Modeling salt intrusion in the San Francisco Estuary prior to anthropogenic influence. Cont Shelf Res. [accessed 2019 Sep 14];146(Supplement C):58–81. *https://doi.org/10.1016/j.csr.2017.07.010*

Berg N, Hall A. 2017. Anthropogenic warming impacts on California snowpack during drought. Geophys Res Lett. [accessed 2019 Sep 14];44(5):2511–2518. *https://doi.org/10.1002/2016gl072104*

Bryant ME, Arnold JD. 2007. Diets of age–0 striped bass in the San Francisco Estuary, 1973–2002. Calif Fish Game. 93(1):1–22.

Casulli V, Stelling GS. 2011. Semi-implicit subgrid modelling of three-dimensional free-surface flows. Int J Num Meth Fluids. [accessed 2019 Sep 14];67(4):441–449. *https://doi.org/10.1002/fld.2361*

Casulli V, Walters RA. 2000. An unstructured grid, three-dimensional model based on the shallow water equations. Int J Num Meth Fluids. [accessed 2019 Sep 14];32(3):331–348. *https://doi.org/10.1002/(sici)1097-0363(20000215)32:3<331::aid-fld941>3.0.co;2-c*

[CDFW] California Department of Fish and Wildlife. 2018. Franks Tract futures? Multi-benefit restoration synthesis report. June 2018. [accessed 2018 Nov 16]; 56 p. Available from: *https://www.wildlife.ca.gov/Conservation/Watersheds/DCF#41062618-franks-tract-restoration-feasiblity*

[CDWR] California Department of Water Resources. 2017. 2015 Emergency drought barrier water quality monitoring report. 161 p.

[CDWR] California Department of Water Resources. 2018. Franks Tract restoration feasibility study using Bay–Delta SCHISM.

[CNRA] California Natural Resources Agency. 2016. Delta Smelt resiliency strategy. [accessed 2018 August 25]; 13 p. Available from: *http://resources.ca.gov/docs/Delta-Smelt-Resiliency-Strategy-FINAL070816.pdf*

Dahm CN, Parker AE, Adelson AE, Christman MA, Bergamaschi BA. 2016. Nutrient dynamics of the Delta: effects on primary producers. San Franc Estuary Watershed Sci. [accessed 2019 July 31];14(4). *https://doi.org/10.15447/sfews.2016v14iss4art4*

Downing BD, Bergamaschi BA, Kendall C, Kraus TEC, Dennis KJ, Carter JA, Von Dessonneck TS. 2016. Using continuous underway isotope measurements to map water residence time in hydrodynamically complex tidal environments. Environ Sci Technol [accessed 2019 Sep 14];50(24):13387–13396. *https://doi.org/10.1021/acs.est.6b05745*

Dugdale R, Wilkerson F, Parker AE, Marchi A, Taberski K. 2012. River flow and ammonium discharge determine spring phytoplankton blooms in an urbanized estuary. Estuar Coast Shelf Sci [accessed 2019 Sep 14];115:187–199. *https://doi.org/10.1016/j.ecss.2012.08.025*

Durand J. 2015. A conceptual model of the aquatic food web of the upper San Francisco Estuary. San Franc Estuary Watershed Sci. [accessed 2019 July 31];13(3). *https://doi.org/10.15447/sfews.2015v13iss3art3*

Fischer HB, List JE, Koh R, Imberger J, Brooks NH. 1979. Mixing in inland and coastal waters. San Diego (CA): Academic Press.

Glibert PM, Dugdale RC, Wilkerson F, Parker AE, Alexander J, Antell E, Blaser S, Johnson A, Lee J, Lee T, et al. 2014. Major—but rare—spring blooms in 2014 in San Francisco Bay Delta, California, a result of the long-term drought, increased residence time, and altered nutrient loads and forms. J Exp Mar Biol Ecol. [accessed 2019 Sep 14];460(0):8–18. *https://doi.org//10.1016/j.jembe.2014.06.001*

Hartman R, Brown L, Thompson J, Parchaso F. 2017. Conceptual model for invasive bivalve control on wetland productivity. In: Sherman, S, Hartman R, Contreras D, editors. 2017. Effects of tidal wetland restoration on fish: a suite of conceptual models. IEP Technical Report 91. Sacramento (CA): California Department of Water Resources. p. 225–258.

Jassby AD, Kimmerer WJ, Monismith SG, Armor C, Cloern JE, Powell TM, Schubel JR, Vendlinski TJ. 1995. Isohaline position as a habitat indicator for estuarine populations. Ecol Appl. [accessed 2019 Sep 14];5(1):272–289. *https://doi.org/10.2307/1942069*

Kayfetz K, Kimmerer W. 2017. Abiotic and biotic controls on the copepod *Pseudodiaptomus forbesi* in the upper San Francisco Estuary. Mar Ecol Progr Ser. [accessed 2019 Sep 14];581:85–101. *https://doi.org/10.3354/meps12294*

Kendall C, Young MB, Silva SR, Kraus TEC, Peek S, Guerin M. 2015. Tracing nutrient and organic matter sources and biogeochemical processes in the Sacramento River and Northern Delta: proof of concept using stable isotope data. U.S. Geological Survey, Data Release 2015, 110. *http://doi.org/10.5066/F7QJ7FCM*

Kimmerer WJ, Gartside E, Orsi JJ. 1994. Predation by an introduced clam as the probable cause of substantial declines in zooplankton in San Francisco Bay. Mar Ecol Progr Ser. [accessed 2019 Sep 14];113:81–93. *https://doi.org/10.3354/meps113081*

Kimmerer WJ, Gross ES, MacWilliams ML. 2014. Tidal migration and retention of estuarine zooplankton investigated using a particle-tracking model. Limnol Oceanogr. [accessed 2019 Sep 14];59(3):901–906. *https://doi.org/10.4319/lo.2014.59.3.0901*

Kimmerer WJ, Gross ES, Slaughter AM, Durand JD. 2019. Spatial subsidies and local mortality of an estuarine copepod revealed using a box model. Estuaries Coasts. [accessed 2019 Sep 14];42(1):218–236. *https://doi.org/10.1007/s12237-018-0436-1*

Kimmerer WJ, Ignoffo TR, Kayfetz KR, Slaughter AM. 2017. Effects of freshwater flow and phytoplankton biomass on growth, reproduction, and spatial subsidies of the estuarine copepod *Pseudodiaptomus forbesi*. Hydrobiologia. [accessed 2019 Sep 14];807(1):113–130. *https://doi.org/10.1007/s10750-017-3385-y*

Kimmerer WJ, Lougee LA. 2015. Bivalve grazing causes substantial mortality to an estuarine copepod population. J Exp Mar Biol Ecol. 473:53–63. *https://doi.org/10.1016/j.jembe.2015.08.005*

Kimmerer WJ, MacWilliams ML, Gross ES. 2013. Variation of fish habitat and extent of the low-salinity zone with freshwater flow in the San Francisco Estuary. San Franc Estuary Watershed Sci. [accessed 2019 Sep 14];11(4). *https://doi.org/10.15447/sfews.2013v11iss4art1*

Kimmerer WJ, Thompson JK. 2014. Phytoplankton growth balanced by clam and zooplankton grazing and net transport into the low-salinity zone of the San Francisco Estuary. Estuaries Coasts [accessed 2019 Sep 14];37(5):1202–1218. *https://doi.org/10.1007/s12237-013-9753-6*

Lee J, Parker AE, Wilkerson FP, Dugdale RC. 2015. Uptake and inhibition kinetics of nitrogen in *Microcystis aeruginosa*: Results from cultures and field assemblages collected in the San Francisco Bay Delta, CA. Harmful Algae. [accessed 2019 Sep 14];47:126–140. *https://doi.org/10.1016/j.hal.2015.06.002*

Lehman PW, Boyer G, Satchwell M, Waller S. 2008. The influence of environmental conditions on the seasonal variation of *Microcystis* cell density and microcystins concentration in San Francisco Estuary. Hydrobiologia. [accessed 2019 Sep 14];600(1):187–204. *https://doi.org/10.1007/s10750-007-9231-x*

Lehman PW, Marr K, Boyer GL, Acuna S, Teh SJ. 2013. Long-term trends and causal factors associated with *Microcystis* abundance and toxicity in San Francisco Estuary and implications for climate change impacts. Hydrobiologia. [accessed 2019 Sep 14];718(1):141–158. *https://doi.org/10.1007/s10750-013-1612-8*

Lopez CB, Cloern JE, Schraga TS, Little AJ, Lucas LV, Thompson JK, Burau JR. 2006. Ecological values of shallow-water habitats: Implications for the restoration of disturbed ecosystems. Ecosystems. [accessed 2019 Sep 14];9(3):422–440. *https://doi.org/10.1007/s10021-005-0113-7*

Lucas LV, Thompson JK. 2012. Changing restoration rules: Exotic bivalves interact with residence time and depth to control phytoplankton productivity. Ecosphere. [accessed 2019 Sep 14];3(12):1–26. *https://doi.org/10.1890/ES12-00251.1*

Luo LF, Apps D, Arcand S, Xu HT, Pan M, Hoerling M. 2017. Contribution of temperature and precipitation anomalies to the California drought during 2012–2015. Geophys Res Lett. [accessed 2019 Sep 14];44(7):3184–3192. *https://doi.org/10.1002/2016gl072027*

MacWilliams ML, Ateljevich ES, Monismith SG, Enright C. 2016. An overview of multi-dimensional models of the Sacramento–San Joaquin Delta. San Franc Estuary Watershed Sci. [accessed 2019 July 30];14(4). *https://doi.org/10.15447/sfews.2016v14iss4art2*

Paerl HW, Huisman J. 2008. Climate-blooms like it hot. Science [accessed 2019 Sep 14];320(5872):57–58. *https://doi.org/10.1126/science.1155398*

Roos M. 1989. Possible climate change and its impact on water supply in California. Oceans. 89:247–249.

R Development Core Team. 2015. R: a language and environment for statistical computing. Vienna: R Foundation for Statistical Computing. Available from: *http://www.R-project.org*

Skrzypek G, Mydlowski A, Dogramaci S, Hedley P, Gibson JJ, Grierson PF. 2015. Estimation of evaporative loss based on the stable isotope composition of water using hydrocalculator. J Hydrol [accessed 2019 Sep 14];523:781–789. *https://doi.org/10.1016/j.jhydrol.2015.02.010*

Slater SB, Baxter RD. 2014. Diet, prey selection, and body condition of age–0 Delta Smelt, *Hypomesus transpacificus*, in the upper San Francisco Estuary. San Franc Estuary Watershed Sci. [accessed 2019 July 31];12(3). *https://doi.org/10.15447/sfews.2014v12iss3art1*

Sobczak WV, Cloern JE, Jassby AD, Cole BE, Schraga TS, Arnsberg A. 2005. Detritus fuels ecosystem metabolism but not metazoan food webs in San Francisco estuary's freshwater Delta. Estuaries. [accessed 2019 Sep 14];28(1):124–137. *https://doi.org/10.1007/BF02732759*

Stewart IT, Cayan DR, Dettinger MD. 2005. Changes toward earlier streamflow timing across western North America. J Climate. [accessed 2019 Sep 14];18(8):1136–1155. *https://doi.org/10.1175/JCLI3321.1*

Ustin S, Khanna S, Bellvert J, Boyer JD, Shapiro K. 2016. Impact of drought on submerged aquatic vegetation (SAV) and floating aquatic vegetation (FAV) using AVIRIS-NG airborne imagery. Sacramento (CA): Calif. Dept. of Fish and Wildlife.

Wilkerson FP, Dugdale RC, Parker AE, Blaser SB, Pimenta A. 2015. Nutrient uptake and primary productivity in an urban estuary: using rate measurements to evaluate phytoplankton response to different hydrological and nutrient conditions. Aquat Ecol [accessed 2019 Sep 14];49(2):211–233. *https://doi.org/10.1007/s10452-015-9516-5*

NOTES

Wells B. 2019. Email to W. Kimmerer about benthic monitoring on June 11.